Noora Tujunen

Amperometric measurement of glutamate

School of Electrical Engineering

Thesis submitted for examination for the degree of Master of Science in Technology.

Espoo 27.5.2013

Thesis supervisor:

Prof. Tomi Laurila

Thesis advisor:

D.Sc. (Tech.) Emilia Kaivosoja

Aalto University
School of Electrical
Engineering

ALTO UNIVERSITY
SCHOOL OF ELECTRICAL ENGINEERING

ABSTRACT OF THE
MASTER'S THESIS

Author: Noora Tujunen

Title: Amperometric measurement of glutamate

Date: 27.5.2013 Language: English Number of pages:8+72

Department of Electronics

Professorship: Microsystems technology Code: S-113

Supervisor: Prof. Tomi Laurila

Advisor: D.Sc. (Tech.) Emilia Kaivosoja

Glutamate is the most abundant neurotransmitter in the mammalian central nervous system. Dysfunction in its regulation has been linked to such medical conditions as Alzheimer's disease, schizophrenia, and Parkinson's disease. In addition to alleviation or elimination of the related symptoms effective treatment for these diseases requires also monitoring the levels of glutamate and other neurotransmitters in the brain.

Electrochemical methods have been widely accepted as an effective method for the detection of neurotransmitters. Amperometric biosensors have been shown to possess suitable characteristics for detection of electroinactive neurotransmitters, such as glutamate and acetylcholine. This, however, requires the immobilization of specific enzyme on the electrode surface.

In this work both self-made and commercial amperometric biosensors were tested in *in vitro* conditions. The sensors were characterized with optical microscopy and scannign electron microscopy. Experiments were conducted in either stationary solutions in a beaker or in a custom made flow cell system. In addition to the response in both glutamate and ascorbic acid containing solutions the effect of temperature was also examined.

The results showed that the conducting the experiments in 37 °C results in higher response when compared to room temperature. The results also indicate that the development of functional layers for amperometric biosensors is not a straightforward process. This is at least mainly due to the non-uniformity of the coating and its poor adhesion on platinum surface. In addition, the experiments with the commercial sensors showed that it is important to consider whether the sensor is optimized to work in *in vivo* or *in vitro*.

Keywords: Amperometry, Biosensors, Enzymes, Glutamate, Neurotransmitters

AALTO-YLIOPISTO
SÄHKÖTEKNIIKAN KORKEAKOULU

DIPLOMITYÖN
TIIVISTELMÄ

Tekijä: Noora Tujunen

Työn nimi: Glutamaatin amperometrinen mittaaminen

Päivämäärä: 27.5.2013 Kieli: Englanti Sivumäärä:8+72

Elektroniikan laitos

Professuuri: Mikrosysteemitekniikka Koodi: S-113

Valvoja: Prof. Tomi Laurila

Ohjaaja: TkT Emilia Kaivosoja

Glutamaatti on yleisin hermovälittäjäaine nisäkkäiden keskushermostossa. Häiriöt sen säätelyssä on liitetty useisiin neurologisiin sairauksiin, kuten Alzheimerin tautiin, skitsofreniaan ja Parkinsonin tautiin. Näihin sairauksiin liittyvien oireiden lievittämiseen tai poistamiseen käytettävien menetelmien lisäksi tehokas hoitaminen vaatii myös glutamaatin ja muiden hermovälittäjäaineiden pitoisuuksien seuraamista aivoissa.

Sähkökemiallisia menetelmiä on käytetty laajalti hermovälittäjäaineiden tunnistamisessa. Amperometriset bioanturit soveltuvat hyvin sähköisesti inaktiivisten hermovälittäjäaineiden, kuten glutamaatin ja asetyylikoliinin, havaitsemiseen. Tämä vaatii kuitenki spesifisten entsyymien immobilisointia elektrodin pinnalle.

Tässä työssä tutkitti sekä itse valmistettujen että kaupallisten amperometristen bioanturien toimintaa *in vitro* olosuhteissa. Anturien rakenteelliseen tutkimiseen käytettiin optista mikroskopiaa ja pyyhkäisyelektronimikroskopiaa. Mittaukset suoritettiin sekoittamattomissa liuoksissa dekantterilasissa tai erikoisvalmisteisessa virtauskammiosysteemissä. Erilaisten glutamaatti- ja askorbiinihappokonsentraatioiden lisäksi myös lämpötilan vaikutus pyrittiin selvittämään.

Kokeet osoittivat, että anturien vaste on korkeampi 37 °C:ssa kuin huoneenlämmössä. Lopputuloksista on lisäksi pääteltävissä, että toimintakykyisten pinnoituskerrosten kehittäminen amperometrisille bioantureille ei ole yksioikoista. Tämä johtuu haasteista valmistaa yhtenäinen pinnoite sekä pinnoitteen heikosta adheesiosta platinapintaan. Lisäksi kaupallisilla antureilla suoritettujen mittausten perusteella voidaan sanoa, että kehitystyössä kokeita suunniteltaessa on huomioitava onko käytettävä anturi optimoitu toimimaan *in vivo* vai *in vitro*-ympäristössä.

Avainsanat: Amperometria, Bioanturit, Entsyymit, Glutamaatti, Hermovälittäjäaineet

Preface

I would like to thank both my supervisors in the process professor Tomi Laurila and professor Mervi Paulasto-Kröckel for the opportunity to work with such an interesting topic. In addition, I would like to thank my instructor Emilia Kaivosoja for all the supportive comments and excellent advice.

A special thanks goes to Rohit Sood for the collaboration in the preparation of the biosensors.

There have also been many others who have greatly helped me with their contribution, and they all deserve to be mentioned here. Olli Kotiranta designed and prepared the flow cell system and conducted some initial experiments with the first set of Pinnacle sensors, Betti Valmari wrote the instructions for how to operate the equipment, Vesa Vuorinen kindly aided me with SEM imaging, and Lasse Rasinen gave me some technical support with LaTeX. In addition, Shaheen Latif and Peter Petillo from Pinnacle Technology Inc. provided me with very uselful information concerning their sensors.

Moreover, writing this would have been a lot more boring without the peer support from Tommi and lunches with Antti.

Finally, I would like to thank also Saana, Heini, Katja, Riku, Tapani, Unto, and of course mum for giving me the best support one can ask for.

Otaniemi, 27.5.2013

Noora Tujunen

Contents

Symbols and abbreviations

Symbols

α_{i}	Proportionality constant for species i
α_{transf}	Dimensionless transfer coefficient
A	Analyte
a_i	Activity of species i
β	Ratio between r_0 and r_1
$C_{\infty,i}$	Bulk concentration of species i
C_d	Double-layer capacitance
C_i^{I}	Concentration of species i before t_f
C_i^{II}	Concentration of species i after t_f
D_i	Diffusivitiy for species i
E	Potential in Ohm's law
E°	Standard potential
E_2	Final potential in the step experinments
E_1	Initial potential in the step experiments
$E^{O'}$	Oxidizing potential
E_R	Reduction potential
e_Σ	Amount of enzyme inside the coating layer
Φ	Potential
F	Faraday's constant
i_f	Current during forward step
i_r	Current during reversal step
i_{SS}	Steady-state current
i_{QSS}	Quasi-steady-state current
J_i	Flux of species i
j	Current density
j_0	Exchange current density
k	Rate constant for oxidation
k_{cat}	Turnover number
K_i	Michaels constant for species i
K_M	Michaelis constant
l	Thickness
m_i	Mass-transfer coefficient for species i
η	Total overpotential
n	Amount of substance in moles
O	Oxidized species
Q	Total charge
R	Reduced species
$R\omega$	Resistance
R_Ω	Compensated resistance
R_S	Solution resistance
R_u	Uncompensated resistance

$\overline{R}$	Gas constant
r_0	Disk or cylinder radius
r_1	Electrode radius including deposited layers
r_{crit}	Critical dimension of an ultamicroelectrode
θ'	Ratio between concentrations of two substances
θ_{i}	Partition coefficient for specie i
τ	Dimensionless parameter for determining the transition region
τ_{tc}	Cell time-constant
T	Temperature
t	Time
t_f	Time for forward part in double-step chronoamperometry
t_r	Time for reversal part in double-step chronoamperometry
t_{step}	Step width in double-step chronoamperometry
W	Electrode area
w	Width of a band electrode
ξ	Square root of the ratio between two diffusion coefficients
x_1	Thickness of inner Helmholtz plane
x_2	Thickness of outer Helmholtz plane
z	Number of electrons transfferred in the reaction

Abbreviations

AA	Ascorbic acid
ATP	Adenosine triphosphate
CE	Capillary electroforesis
DHA	Dehydroascorbic acid
DKG	Diketogulonate
GABA	γ-aminobutyric acid
Glu	Glutamate
GluOx	Glutamate oxidase
IHP	Inner Helmholtz plane
pmPD	poly(m-phenylenediamine)
NMDA	N-methyl-D-aspartate
NO	Nitric oxide
OHP	Outer Helmholtz plane
UME	Ultramicroelectrode

1 Introduction

The origins of the several neurological conditions, such as Parkinson's disease, schizophrenia, and Alzheimer's disease, have been linked to the dysfunction of neurotransmitters. These signalling molecules in the central nervous system can either excite or inhibit neurons resulting in effective but also complex internal communication. Detecting the molecules in the brain would provide means to develop methods to improve the quality of life of patients suffering from the previously mentioned diseases.

In addition to medication since the 1990's it has been possible to utilize a method called deep brain stimulation in the treatment of for example Parkinson's disease or essential tremor [1, 2]. This approach includes chronically implanting electrodes in brain of the patient and stimulating certain regions with electric currents to alleviate the symptoms of the disease. What is still lacking is the ability to monitor the brain activity continuously during the *in vivo* life time of the device. Developing means to this would provide access to feedback control to further improve the efficiency of the treatment.

Electrochemisty is a branch of chemistry focused on the phenomena related to both electrical and chemical reactions [3, p.1]. Depending on the system it is possible to measure either currents or voltages as a function of the other or time. Amperometry is a method were currents are measured as a function of time whereas voltammetry is concerned with current behaviour as a function of voltage. In addition to fundamental research, different electrochemical techniques have been widely studied as a tool for detecting neurotransmitters both *in vitro* and *in vivo*.

An important property of neurotransmitters related to their detection by electrochemical methods is their electroactivity. Substances such as dopamine and serotonin can be readily oxidised on electrode surface, and the resulting current can be used in their detection. However, electroinactive molecules, such as glutamate and acetylcholine, have to be first transformed into electrochemically detectable species, typically H_2O_2. This involves coating the electrode surface with enzyme-containing layers. Devices relying on such biorecognition element are called biosensors. In addition to the enzyme coating other layers are usually deposited on neurotransmitter sensors in order to block different interfering species, such as ascorbic acid (AA), and reduce biofouling of the electrodes.

In this master's thesis work the properties of self-made and commercial amperometric biosensors were examined. The results indicate that the coatings on the self-made electrodes may not have been properly adhered on the electrode surfaces, and it was not possible to measure glutamate in a reliable way. On the other hand, the experiments with the commercial sensors the relevance of sensors being optimized for either *in vitro* or *in vivo* conditions. In addition, with both self-made and commercial sensors higher response was obtained in experiments conducted in 37 °C than in room temperature.

The work has been divided into 7 sections. After the introduction, electrochemical methods and neurotransmitters are reviewed separately in sections 2 and 3. Section 4 is focused on the biosensors applications for neurotransmitter detection.

After the literature review the purpose of the work is summarized in section 5. Materials and methods used in this work are presented in section 6 followed by the description of the obtained results with some suggestions for future directions in section 7. Finally, the section 8 presents the conclusions based on the earlier chapters and the experimental work.

2 Electrochemical methods

Electrochemistry is a branch of chemistry where the interest lies in the study of electrical and chemical effects and their relations. In an electrochemical system the electrode can be seen as analogous to either oxidizing or reducing agent depending on the direction of the flowing current. This direction is determined by the electrode potential: for positive values the electrons flow from the solution to the electrode resulting in the oxidation of the species in the electrolyte. For negative values the current flow in the opposite direction and the reaction occurring at the electrode is reduction. However, it is important to keep in mind that the here terms positive and negative potential are not ambiguous. Each substance has its own oxidation and reduction potentials depending on its nature. At certain potential an equilibrium will be eventually reached between oxidized and reduced species. In electrochemical measurements the center of attention is the flow of the current that occurs as the reaction moves towards equilibrium. The current density is directly proportional to the rate of the reaction occurring at the surface of the electrode, and therefore the difference in the reaction kinetics can be applied in determining the identities of different substances. [4]

2.1 Electrochemical systems

When examining an electrochemical system the focus is in the factors affecting charge transport between chemical phases. These phases can be, for example, a metallic electrode and a liquid electrolyte in which the electrode is immersed. The electrochemical events of interest, i.e. reduction and oxidation of the participating chemical species, occur at the electrode/electrolyte interface according to equation (1):

$$Oxidized\ form + ne^- \leftrightharpoons Reduced\ form, \tag{1}$$

where n is the number of electrons transferred in the reaction. In this work the oxidized and reduced forms will be marked with O and R, respectively. The reaction depicted in equation (1) requires that there exists a potential difference across the interface and a current passes through it. It is obvious that both electrode and electrolyte have to be conducting. In the electrode the movement of electrons results in charge transfer, whereas in the electrolyte it is the movement of ions that carries the charge.

2.1.1 Electrodes in electrochemical systems

In order to experimentally examine the electrochemical phenomena, the minimum requirement is a system of at least two electrodes and one electrolyte phase separating them, i.e. an electrochemical cell. The term half reaction refers to the reactions that occur at one of the electrodes and the overall chemical reaction can be defined as the sum of the half-reactions in the electrochemical cell. By measuring the potential difference between the electrodes, i.e. the cell potential, it is possible

to determine the direction and rate of charge transfer at the interface of interest. However, as it is impossible to experimentally examine the half-cell potential of only one electrode, electrodes of constant composition and thus also constant potential are used as reference electrodes. Common reference electrodes are the standard hydrogen electrode, saturated calomel electrode and silver-silver chloride (Ag/AgCl) electrode. The electrode at which the reactions take place is called the working electrode and its potential is quoted with respect to the used reference electrode. The reduction potential value against the standard hydrogen electrode is called the standard potential, E°, and it can be substituted in the Nernst equation (2) to determine the reduction potentia (E_R) of a half-cell reaction at equilibrium:

$$E_R = E^{\circ} + \frac{\overline{R}T}{zF} \ln(\frac{a_O}{a_R}), \tag{2}$$

where $\overline{R}$ is the gas constant, T the temperature in Kelvin, z the number electrons transferred in the reaction, F the Faraday constant, and a_i the activity of the species participating in the reaction. In electrochemistry it is also common to replace the activities a_i with concentrations. Systems following the Nernst equation are said to be thermodynamically or electrochemically reversible.

Ultramicroelectrodes

Historically, the term microelectrode has been used to describe electordes operating under such conditions that the electrochemical reaction does not affect the bulk concentrations of the electroactive species [3, p. 156]. This can be obtained by having the solution volume large enough compared to the electrode surface area. However, the development of electrodes with dimensions in the micro or even nano scale has resulted in the term "microelectrode" becoming ambiguous as some authors have started to use it in reference of the very small electrodes. It is of course correct to do so as these electrodes definitely satisfy the small A/V conditions but as the term can also refer to much larger electrodes the micro and nanoscale electrodes have often been called "ultramicroelectrodes" (UME) in order to avoid the confusion. Even though there is no widely accepted consensus on the definition of ultramicroelectrodes, it is generally agreed that the electrode should be smaller than the diffusion layer developed in readily achievable experiments [3, p.169]. However, to produce the characterstic UME properties only one electrode dimension, i.e. the critical dimension r_{crit}, has to be small. This makes various different shapes available for different types of UME applications. In addition to the most common disk UMEs it is also possible to fabricate spherical, hemispherical, band and cylindrical UMEs.

2.2 Experimental setups in electrochemistry

In electrochemical systems it is impossible to simultaneously control the potential and the current. This implies that there are altogether three possible basic exper-

imental setups: measuring the potential when the current is zero, measuring the potential while controlling the current, and measuring the current while controlling the potential. All mentioned setups are based on Ohm's law (3):

$$E = iR_{\omega}. \tag{3}$$

In other words, the current i passing through resistance R_{ω} generates the potential E. Different experimental configurations require different equipment. A potentiometer is an instrument that measures the potential in the case where the current is zero. As no current flows, also no net faradaic reactions occur, and the potential is mainly based on the thermodynamic properties of the system [3, p. 19]. A galvanostat lets the experimenter control the current flowing through the cell. Even though the setup is typically more simple than for controlled potential instrumentation the drawback in controlled current experiments is that the the effect of charging current of the double-layer is larger. It occurs throughout the whole measurement which makes correcting for it challenging. In multicomponent systems and stepwise reactions the data analysis can be even more difficult [3, p. 306]. Controlling the potential of the working electrode is possible with an instrument called a potentiostat. The potential is measured against the reference electrode which is held at constant potential. The potential can be adjusted by changing the resistance between the working and auxiliary electrodes.

The electrode reaction rate and the detected current are affected by such factors as the mass-transfer of the reacting species from the bulk to the electrode, electron transfer at the electrode surface, homogenous or heterogeneous chemical reactions preceding or following electron transfer, and various surface reactions, including adsorption, desorption, and crystallization. As some of these reactions are more sluggish than the others the rate of the overall reaction depends on the rate of the slowest processes. These are called the rate-determining steps. The total overpotential η, i.e. the extent of electrode potential departure from the equilibrium value, resulting in certain current density j is a sum of the overpotentials of each contributing reaction. [3, p. 22-24] Relation between η and the j can be expressed according to the Butler-Volmer equation (4 [3, p.100]:

$$j = j_0\left[e^{\frac{-\alpha_{transf}F\eta}{RT}} - e^{\frac{(1-\alpha_{transf})F\eta}{RT}}\right], \tag{4}$$

where j_0 is the exchange current density and α_{transf} is dimensionless transfer coefficient. Derivation for the equation can be found from most books concerning the theory of electrochemistry.

The electrochemical techniques can be divided into static and dynamic techniques. In static techniques, e.g. potentiometry, no current flows through the cell and the potential under these conditions is measured. Here, however, we are more interested in the dynamic techniques and especially the controlled potential setups owing to their wide application in the neurotransmitter related research. In detecting neurotransmitters commonly used electrochemical techniques include constant-potential amperometry, chronoamperometry, differential pulse voltammetry and fast

scan cyclic voltammetry [5]. In this work the focus is on the amperometric methods for they are often combined with enzymatic biosensors.

It is, however, noteworthy that the use of electrochemical methods in neuroscience is limited to the study of dynamic events, such as secretion of neurotransmitters arising from certain stimulus. This is due to the charging current that is usually impossible to distinguish from the Faradaic current in static conditions, i.e. measuring the resting or basal concentrations of the target substances [4]. Oxidation and reduction taking place at the electrode surface are caused by charge transfer over the electrode/electrolyte interface. Since the relation between the amount of chemical reaction and the flow of current can be modeled by Faraday's law (see equation (5)) stating that the transfer of one electron results in production or consumption of 1 mole of product or reactant, respectively, these reactions are called faradaic processes.

$$it = Q = znF, \tag{5}$$

where t is time, Q is the total charge transferred, and n is the amoun of substance in moles. On the contrary, when there is no charge transfer over the interface such non-faradaic processes as adsorption and desorption can change the potential and the solution composition which results in the flow of external currents. One of these currents arises from the rearrangement of the ions in the solution and it is called the charging current. In real systems both faradaic and non-faradaic processes occur although there are some electrodes that exhibit charge transfer only at quite negative potentials allowing their treatment as ideally non-faradaic over certain potential range. For such electrodes the electrode-electrolyte interface resembles a capacitor since charge cannot cross from one phase when the potential is changed.

2.3 Mass-transfer

In all electrode applications one important aspect is also the mass-transfer of the reacting molecules to the electrode. Basically, mass-transfer can be described as the movement of material from one location to another. Its three modes are migration, diffusion and convection. Migration arises from a gradient of electrical potential and it involves a charged body moving in an electric field wheres diffusion occurs as a result of a concentration gradient or chemical potential gradient formed between two locations of the system. Convection can be either natural arising from density gradients or forced like for example in the case of stirring the solution. One-dimensional mass-transfer along the x-axis is governed by the Nerns-Planck equation (6):

$$J_i(x) = -D_i \frac{\partial C_i(x)}{\partial x} - \frac{zF}{RT} D_i C_i \frac{\partial \Phi(x)}{\partial x} + C_i v(x), \tag{6}$$

where J_i, D_i, and C_i are the flux, diffusivity and concentration of species i, respectively. Φ denotes the potential and v the velocity with which a volume element in solution moves along the axis. In electrochemical setups the system is often designed so that migration and convection can be avoided in order to simplify the

otherwise complex solution for the flux. By using a supporting electrolyte at a concentration much larger compared to the concentration of the electroactive species in the solutions migration can be reduced to negligible level. Minimizing the effect of convection is possible by preventing stirring and vibration of the solution. [3, p. 28]

2.4 The electrical double-layer

At equilibrium there is no electric field within a metal electrode, and all of the excess charge is accumulated at the surface. On the other hand, as it is impossible for negative or positive charge to exist alone the counter-ions in the solutions also reside in the vicinity of the electrode surface. These sheets of opposite charge form so called double-layer first described by Helmholtz - hence the name Helmholtz model [3, p. 544]. The limitation of the Helmholtz model is, however, that it assumes the differential capacitance of the layer is constant. This weakness in the model can be handled by including a diffuse layer of charge in the solution in addition to the inner layer, i.e. compact or Helmholtz layer. The inner layer contains solvent molecules and other species, such as ions or molecules, that are specificially adsorbed. The thickness of diffuse layer depends on the total ionic concentration of the solution, and for concentrations greater than 10^{-2} M it is less than 100 Å [3, p.13]. As the electrode charge increases the layer becomes more compact resulting in rising values for the differential capacitance. Similar effect can be observed when there is an increase in the solution concentration. This model was proposed by Gouy and Chapman, thus it is called the Gouy-Chapman theory. In the Gouy-Chapman model the ions are considered as point charges which can be located arbitrarily close to the surface. At high polarization the diffuse layer decreases continuously towards zero, and the differential capacitance increases towards infinity. However, it is obvious that in real situations this is not the case since the ions have non-zero radius. The radius determines the closest distance they can approach from the surface. Furthermore, for ions that remain solvated also the thickness of the primary solution sheat should be added to the total distance. The so-called Stern's modification provides solutions for this problem by expanding the original Gouy-Chapman theory [3, p. 546]. For low electrolyte concentrations the thickness of the diffuse layer is large compared to the distance of the centers of the solvated ions from the electrode surface, x_2. This region x_2 in the diffuse layer is also called the outer Helmholtz plane (OHP). Increasing the polarization or the electrolyte concentration compresses the charge more tightly against the boundary at distance x_2 so that finally the system can be described according to the original Helmholtz model.

In OHP the molecules have only long-range interactions with the electrode surface. However, between the surface and OHP there is a region called the inner Helmholtz plane (IHP) where the molecules are specifically adsorbed and in addition to short-range electrostatic force affecting them they can also have chemical interactions with the surface. The thickness of IHP, x_1, can be determined between the surface and the electrical centers of the specifically adsorbed molecules. [6, p. 66]. The whole scheme with both inner and oute Helmholtz planes is summarized in Fig. 2.4.1.

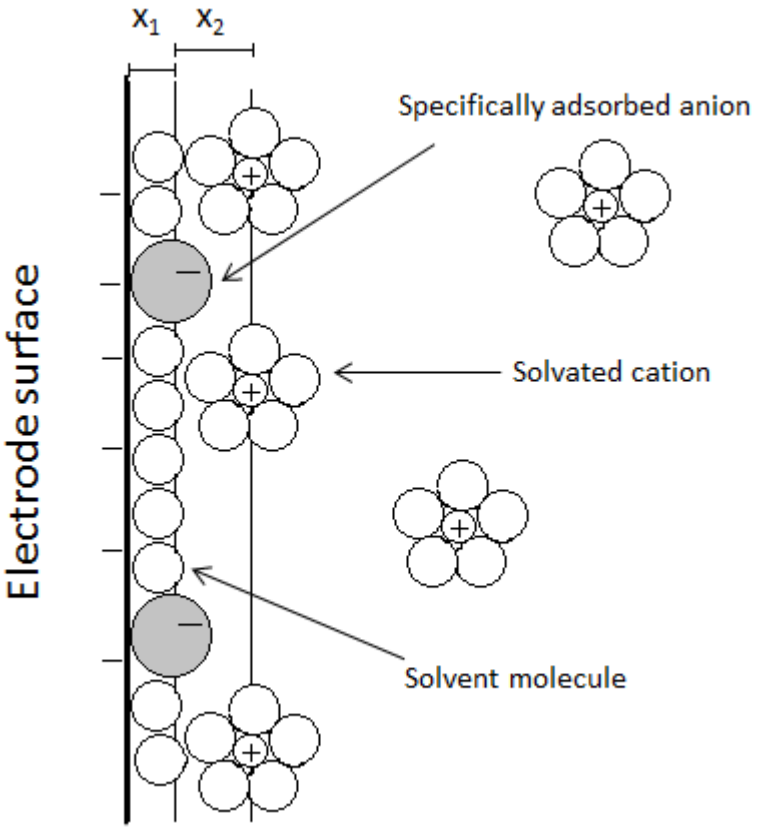

Figure 2.4.1: Schematic illustration of the electrical double layer. x_1 and x_2 mark the lengths of inner and outer Helmholtz planes, respectively. (Drawn after [3, p.13].)

It is noteworthy that the charge density in the solution side of the interface is divided between the compact layer adjacent to the electrode and the diffuse layer, i.e. between the Helmholtz planes. Furthermore, electroactive species that are not specifically adsorbed can approach the electrode to distance x_2. This means that the potential affecting these species is less than between the solution and the electrode surface. Hence, the double-layer can affect the electrode processes, and it is important to consider its impact on the results obtained from electrochemical experiments. [3, p.13] For example, one implication is that the concentrations for oxidised and reduced species C_O and C_R, respectively, reside in the OHP.

2.5 Amperometry

Amperometry is an electrochemical technique where the potential at the working electrode is held constant respect to a reference electrode and the interest is in the obtained current vs. time data. At low currents (10^{-9} to 10^{-6} A) the reference electrode can also act as the auxiliary electrode [7]. Depending on the substance detected the current is directly correlated to either its bulk concentration or its

generation or consumption within the biocatalytic element containing layer on the electrode [7]. Amperometry provides no information about the current vs. potential properties of the detected substance and thus it is best suited to situations where the identity of the reduced or oxidized species is known [4].

An instrument called potentiostat is used to maintain the potential difference between the working and reference electrodes. It controls the voltage by forcing the needed current through the working electrode. At the electrode the flow of electrons (current) results in electrochemical reactions that have rates consistent with the potential.

Changing the potential to a region where the oxidation (reduction) of the substrate is extremely fast results in the vicinity of the electrode becoming depleted of the substance. This gives rise to a concentration gradient and the substrate molecules start to flow towards the electrode. According to Fick's first law (7) the flux of the substrate, J_O, is proportional to the concentration gradient $\partial C_O/\partial x$:

$$-J_O = D_O \frac{\partial C_O(x)}{\partial x}, \tag{7}$$

where D_O is the diffusivity of the substrate. D_O does not depend on the concentration of the oxidized species. All the substrate that reaches the electrode is instantly oxidized (reduced) and the concentration at the electrode surface remains zero as long as the potential and thus also the flow of electrons is maintained. As the depletion zone of the substrate grows thicker with time also the current decreases. It is said that the electrode reactions are mass-transfer limited since it is the diffusion of the substrate particles from the electrolyte to the electrode surface that controls the rate of oxidation (reduction). Providing that no other electrode reactions take place it is possible to write a relation between the flux of the substrate, the current and the concentration gradient at the electrode:

$$-J_O(0,t) = \frac{i}{zFW} = D_O \Big[\frac{\partial C_O(x,t)}{\partial x}\Big]_{x=0}, \tag{8}$$

where W is the area of the electrode. Stepping the potential back to the initial region results in a large cathodic (anodic) current arising from quick rereduction (reoxidation) of the previously oxidized (reduced) substrate. Also in this case diffusion starts to limit the reaction with time and the growing depletion zone causes the current to decline. An experiment where the potential is first stepped to the mass-transfer limited region then after certain period returned back to the initial value is called double-step chronoamperometry and it belongs to the group of reversal techniques. However, before more detailed description of the double-step method it is more convenient to first approach the current response through the forward step only.

Stepping the potential to a region where the surface concentration of the oxidized form of the substance becomes effectively zero provides means to examine the current-time response qualitatively. In this region the current is mass-transfer i.e. diffusion limited, and calculation of its value involves the solution of the linear

diffusion equation or Fick's second law (9):

$$\frac{\partial C_O(x,t)}{\partial t} = D_O \frac{\partial^2 C_O(x,t)}{\partial x^2}. \tag{9}$$

For equation (9) the following boundary conditions apply:

$$C_O(x,0) = C_{\infty,O} \tag{10}$$

$$\lim_{x\to\infty} C_O(x,t) = C_{\infty,O} \tag{11}$$

$$C_O(0,t) = 0(\text{for t} > 0). \tag{12}$$

Equation (10) defines the initial conditions and the homogeneity of the solution before the experiment. The second boundary equation (11) gives information about the conditions of regions that are distant from the electrode and hence remain unchanged also during the experiment. The last boundary (12) specifies the conditions at the electrode surface after the potential step. Combining the Laplace transformation of equations (8) and (9) under the previously presented boundary conditions results in the current-time response $i_d(t)$:

$$i(t) = i_d(t) = \frac{zFWD_O^{1/2}C_{\infty,O}}{\pi^{1/2}t^{1/2}}. \tag{13}$$

In equation (13), known as the Cottrell equation, the inverse $t^{1/2}$ function is a mark of the diffusion control over the rate of the reaction. It is noteworthy that a non-faradaic current also flows during a potential step. This current decays exponentially according to equation (14):

$$i = \frac{E}{R_S} e^{-t/R_S C_d}, \tag{14}$$

where R_S is the solution resistance and C_d the double-layer capacitance. The solution resistance R_S is composed of two parts, the uncompensated resistance R_u between the reference and working electrodes, and the compensated resistance R_Ω between the reference and auxiliary electrodes. It is possible to define the cell time constant for the system with R_u and C_d: $\tau_{tc} = R_u C_d$. The charging of the double layer and the charging current affect identifying the faradaic current for about a period of five time constants. In addition, in order to apply the assumption of instantaneous redox reactions and the change of surface concentration to zero at the beginning of the experiment the shortest data collection time has to be considerably greater than the time constant.

The previous treatment basically applies for planar electrodes in unstirred conditions where diffusion can be presumed to be linear. However, especially in the case of ultamicroelectrodes the shape of the electrode the diffusion of the substrate to the electrode differs from the linear mode. This will have an effect on the current profiles of the electrodes, and thus also the Cottrell equation takes a different form depending on the electrode geometry. Kotanen *et al.* [8] have provided a summary

of different electrode geometries with their governing equations and schematic illustrations of the varying diffusion fields (Fig. 2.5.1). Note that in the figure the equations have been written for the oxidized species O but they also apply for the reduced species R.

Geometry	Disc electrode	Microdisc electrode	Microdisc electrode array
Image	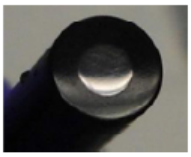		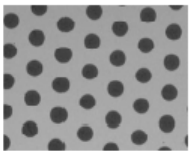
Current profiles	$i(t) = \frac{zFWD_O^{1/2}C_{\infty,O}}{\pi^{1/2}t^{1/2}}$	$i(t) = \frac{zFWD_O^{1/2}C_{\infty,O}}{2\pi^{1/2}t^{1/2}} + \frac{zFWD_O^{1/2}C_{\infty,O}}{2r_0}$	$i(t) = \frac{zFW^{array}D_O^{1/2}C_{\infty,O}}{\pi^{1/2}t^{1/2}}; \frac{d}{r_0} \gg 4$
Applicable conditions	Planar electrode; semi-infinite linear diffusion	Planar electrode, hemispherical diffusion	Array of disc electrodes, multiple domains of diffusion
Steady state current	$i_{SS} = 4zFC_{\infty,O}D_O r_0$	$i_{SS} = 4zFC_{\infty,O}D_O r_0$	$i_{SS} = 4zNFC_{\infty,O}D_O r_0$
Diffusion field	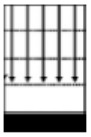	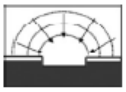	

Geometry	Sphere	Hemisphere	Needle electrode
Image		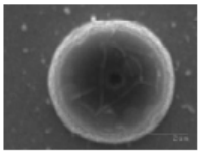	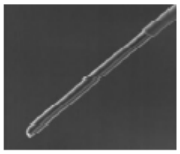
Current profiles	$i(t) = zFWD_O C_{\infty,O}\left(\frac{1}{\pi^{1/2}D_O^{1/2}t^{1/2}} + \frac{1}{r_0}\right)$	$i(t) = zFWD_O C_{\infty,O}\left(\frac{1}{\pi^{1/2}D_O^{1/2}t^{1/2}} + \frac{1}{2r_0}\right)$	$i(t) = \frac{zFWD_O C_{\infty,O}}{r_0}\left(\frac{2\exp(0.05\pi^{1/2}\tau^{1/2})}{\pi^{1/2}\tau^{1/2}} + \frac{1}{\ln(5.2945+0.3)}\right)$
Applicable conditions	Spherical electrode; spherical diffusion	Hemispherical electrode; radial diffusion	Cylindrical electrode; radial diffusion
Steady state current	$i_{SS} = 4\pi zFC_{\infty,O}D_O r_0$	$i_{SS} = 2\pi zFC_{\infty,O}D_O r_0$	$i_{QSS} = \frac{4zFC_{\infty,O}D_O}{r_0 \ln\tau}$
Diffusion field	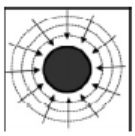	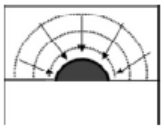	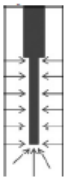

Figure 2.5.1: Different electrode geometries, equations for the current responses and schematic illustrations of the varying diffusion field. In the case of the microdisk array N is the number of microdisks. (Modified from [8].)

However, at short times the diffusion layer thickness remains small compared to the smallest dimension of the electrode and the diffusion can be regarded as linearly semi-infinite. As a conclusion the current profile can be modeled by the original

Cottrell equation (13). At longer times the thickness of the diffusion layer grows thicker and the current at the electrode approached a steady state or a quasi-steady state in the case of cylindrical UME for species R:

$$i_{ss} = zFWm_R C_{\infty,R}, \tag{15}$$

where m_{R} denotes the so-called mass-transfer coefficient. In the case of ultamicroelectrodes the form of m_{R} depends on the shape if the electrode (Table 2.5.1). Since the transition region between the short-time and the long-time regime involves complex theory with no considerable advantages in experimental setups it is common to aim to operate in either of the other regions [3, p. 176]. The transition regime can be defined with a dimensioless parameter $\tau = 4D_R t/{r_0}^2$. For a disk UME τ represents the squared ratio of the diffusion length to the radius of the disk r_0 (or the critical dimension of the UME for other geometries). In the short-time regime the diffusion layer remains small compared to r_0 and τ takes values lower than 0.01. In the intermediate or transition regime the diffusion layer thickness is comparable to r_0, and $0.01 < \tau < 10.00$. Finally, in the steady-state the diffusion layer size is significantly larger than the radius of the disk and $\tau > 10.00$. For an disk UME with r_0 and D_R values of 5 µm and 10^{-5} cm^2/s the time frame for short time is below 60 µs and for intermediate regime between 60 µs and 60 ms. In the long time regime between 60 ms and 60 s the diffusion layer grows in size from 16 µm to 500 µm. [3, p.170-174]

It is noteworthy that the definition of steady-state current for a cylindrical UME presented in Fig. 2.5.1 and equation (15) is actually so-called quasi-steady-state current, i_{qss}. This arises from the current being dependent on time through the previously defined parameter τ. However, it appears only as inverse logarithmic function, and thus in the quasi-steady-state regime the current declines rather slowly with time [3, p. 175]. For simplicity reasons in this work the current is discusses as being the steady-state current but it is important to keep in mind that for cylindrical UMEs it actually means the quasi-steady-state equivalent.

Table 2.5.1: Mass-transfer coefficients for ultramicroelectrodes of different geometries. For cylindrical geometry the long-time limit is quasi-steady state. In the table w is the width of the band electrode. [3, p.176]

Band	Cylinder	Disk	Hemisphere	Sphere
$\frac{2\pi D_R}{w\ln(64D_R t/w^2)}$	$\frac{2D_R}{r_0\ln(\tau)}$	$\frac{4D_R}{r_0}$	$\frac{\pi D_R}{r_0}$	$\frac{D_R}{r_0}$

2.5.1 Constant potential amperometry

In constant-potential amperometry the electroactive species is reduced or oxidized at the electrode surface while the potential is held constant and at sufficient level during the whole experiment to induce the electrochemical reaction (see Fig. 2.5.2).

The integral of the resulting current with respect to time gives the total charge Q. By employing Faraday's law (5) it is possible to obtain the amount of species electrolyzed. The redox reactions occur immediately as the electroactive species arrive at the electrode, and thus the adsorption does not slow down the process. With constant-potential amperometry and sampling rate in the kHz range it is possible to achieve time resolution in the sub-millisecond time scale. However, the requirements for diffusion layer shape and dimensions make it challenging to apply this technique to determine concentrations. In addition, all electroactive species that undergo reduction or oxidation at the potential will contribute to the detected faradaic current. Constant-potential amperometry does not provide any information about identities of the reacting molecules. [5]

2.5.2 Double-step chronoamperometry

In chronoamperometry the electrode is first held at an initial potential where no oxidation or reduction occurs. Stepping the potential into a region where either of these reactions takes place results in the immediate reduction or oxidation of the target substance in contact with the electrode and the development of concentration gradient between the electrode surface and the bulk solution. As the reaction soon becomes diffusion controlled it is possible to apply the Cottrell equation (13) in order to calculate the current-time relationship [4]. Double-step chronoamperometry is a technique where the effect of the initial potential step is usually reversed by second step in potential. Fig. 2.5.2 presents an example considering a case where an electrode is immersed in a solution containing species R which oxidizes at potential $E^{O'}$. Let the initial potential E_1 be more negative than $E^{O'}$. At t = 0 the potential is stepped to value E_2, which is considerably more positive than $E^{O'}$. At this potential species O is generated from R through oxidation for a period t_{step}. At t_{step} a second step is applied to value E_R, which is significantly more negative compared to E_2 and $E^{O'}$ (often $E_R = E_1$). As the potential is now more negative than $E^{O'}$ the oxidized species O can not exist anymore and it reduces back to R.

In order to get quantitative information about the concentration profiles and current behaviour during the reversal step it is common to use the principle of superposition. In other words, the signal can be constructed by superposing a constant component E_2 for all t $>$ 0 and a step component E_R-E_2 for t $>$ t_{step}. Mathematically this can be represented by equation (16)

$$E(t) = E_2 + S_{t_{step}}(t)(E_R - E_f) \qquad (t > 0), \tag{16}$$

where the step function $S_{t_{step}}$(t) equals zero for t $\leq$ t_{step} and unity for t $>$ t_{step}. Superposition can be applied also to express the concentrations of species R and O:

$$C_R(x,t) = C_R^I(x,t) + S_{t_{step}}(t)C_R^{II}(x, t - t_{step}) \tag{17}$$

$$C_O(x,t) = C_O^I(x,t) + S_{t_{step}}(t)C_O^{II}(x, t - t_{step}), \tag{18}$$

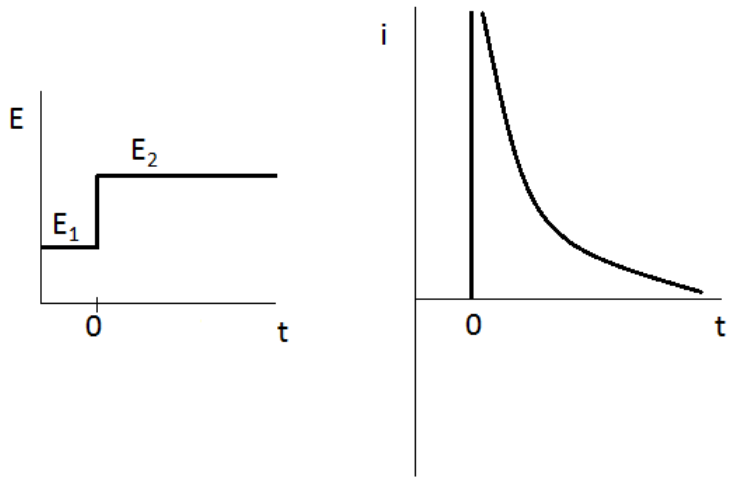

Figure 2.5.2: Effect of a potential step starting at t = 0 (left) and the resulting current response (right). (Drawn after [3, p.157].)

where superscripts I and II denote the concentrations before and after t_{step}, respectively. At $t = 0$ the concentrations of R and O can be written as

$$C_R(x,0) = C_{\infty,R} \qquad C_O(x,0) = 0, \tag{19}$$

where $C_{\infty,R}$ is the bulk concentration of species R. During the forward step the concentrations at the electrode surface become

$$C_R(0,t) = C'_R \qquad C_O(0,t) = C'_O. \tag{20}$$

However, the following treatment is limited to the case where the couple R/O is Nernstian. This allows writing

$$C'_R = C'_O e^{\left[\frac{zF}{RT}(E_2 - E^{O'})\right]}. \tag{21}$$

Equally, the reversal step is defined by

$$C_R(0,t) = C''_R \qquad C_O(0,t) = C''_O \tag{22}$$

and

$$C''_R = C''_O e^{\left[\frac{zF}{RT}(E_R - E^{O'})\right]}. \tag{23}$$

At all times, the following semi-infinite conditions (24) stating that regions distant from the electrode remain unchanged during the course of the experiment and flux balance (25) apply:

$$\lim_{x\to\infty} C_R(x,t) = C_{\infty,R} \qquad \lim_{x\to\infty} C_O(x,t) = 0 \tag{24}$$

$$J_R(0,t) = -J_O(0,t), \tag{25}$$

where J_R and J_O are the fluxes for species R and O, respectively. Equations (21) and (23) restrict the application of this model to cases where the electron transfer is Nernstian. The method of superposition requires that all previous conditions as well as diffusion equations for species R and O are linear. Many electrochemical systems do not meet these requirements and in order to solve the concentration profiles and the current-time relationship other predictive techniques are needed. When linearity and reversibility apply the current during the forward step ($0 < t < t_{step}$) can be expressed as

$$i(t) = i_d(t) = \frac{zFWD_R^{1/2}C_R^*}{\pi^{1/2}t^{1/2}(1+\xi\theta')}, \tag{26}$$

where ξ is the square root of the ratio between the diffusion coefficients of species R and O, and θ' is the ratio between the concentrations of these molecules at the electrode surface:

$$\xi = \sqrt{\frac{D_R}{D_O}} \tag{27}$$

and

$$\theta' = \frac{C_R(0,t)}{C_O(0,t)} = e^{\left[\frac{zF}{RT}(E_2 - E^{O'})\right]}. \tag{28}$$

It is clear that this is of the same form as the Cottrell equation (13). The difference is in the scaling factor $(1 + \xi\theta')^{-1}$. At the diffusion-limited region letting $\theta' \to 0$ the effect of the scaling factor is eliminated and the current takes the form expressed by the original Cottrell equation. The current during the reversal step can be expressed as follows:

$$-i_r(t) = \frac{zFWD_R^{1/2}C_{\infty,R}}{\pi^{1/2}}\left\{\left(\frac{1}{1+\xi\theta'} - \frac{1}{1+\xi\theta''}\right)\left[\frac{1}{(t-t_{step})^{1/2}}\right] - \frac{1}{(1+\xi\theta')t^{1/2}}\right\}. \tag{29}$$

Combining the currents for forward and reversal steps expressed in equations (26) and (29) the resulting response takes the form shown in Fig. 2.5.3.
In the purely diffusion limited case equation (29) simplifies to:

$$-i_r(t) = \frac{zFWD_R^{1/2}C_{\infty,R}}{\pi^{1/2}}\left[\frac{1}{(t-t_{step})^{1/2}} - \frac{1}{t^{1/2}}\right]. \tag{30}$$

As absolute currents are proportional to electrode area W and the square root of the diffusivity of species R ${D_R}^{1/2}$, which can be difficult to determine, comparing real results and the predicted values is often inconvenient. To overcome this it is possible to divide the reversal current, -i_r, by some a certain value of the forward

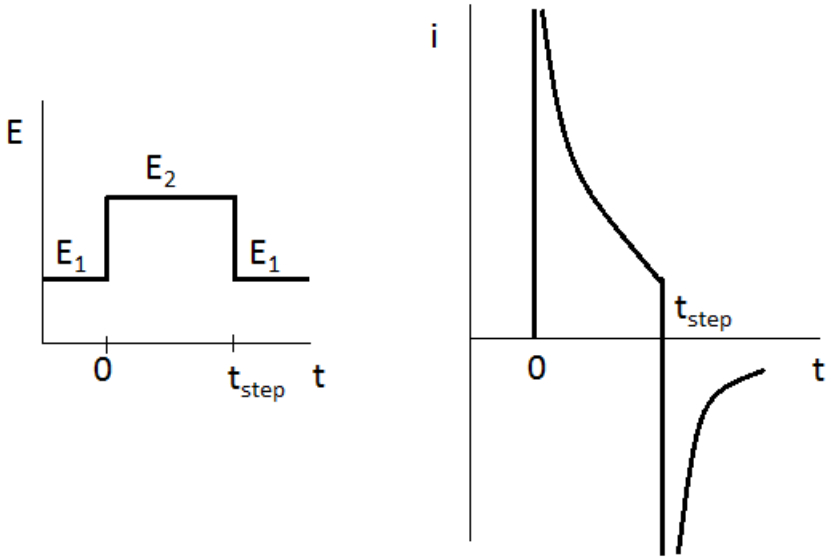

Figure 2.5.3: Schematic illustration of the double-potential step from $t = 0$ to $t = t_{step}$ (left) and the resulting current response (right). (Drawn after [3, p.159].)

current. For the diffusion limited situation taking two instants of time, t_r for the reversal part and t_f for the forward step, results in

$$\frac{-i_r}{i_f} = \left(\frac{t_f}{t_r - t_{step}}\right)^{1/2} - \left(\frac{t_f}{t_r}\right)^{1/2}. \tag{31}$$

Moreover, selecting so that $t_\mathrm{f} = t_\mathrm{r}$ - t_{step} always applies, equation (31) becomes

$$\frac{-i_r}{i_f} = 1 - \left(1 - \frac{t_{step}}{t_r}\right)^{1/2}. \tag{32}$$

This information can be applied to test the stability of the system. For stable systems -$i_\mathrm{r}(2t_{step})/i_\mathrm{f}(t_{step})$ = 0,293 [3, p. 210]. Deviations from this value are an indication of kinetic complications in the electrode reaction. For example, O can decay into electroinactive species, and as the resulting current $|i_\mathrm{r}|$ is smaller than the predicted value given by equation (30), the current ratio -$i_\mathrm{r}/i_\mathrm{f}$ also differs negatively from (32).

One advantage of double-step chronoamperometry is that the ratio of the currents at forward and reverse potential step gives some information about the stability of the oxidized species. This option provides some insight into the chemical identities of the reacting species, even though the selectivity still remains quite low. [5] The advantages and disadvantages of both constant potential and double-step chronoamperometry have been summarized in Table 2.5.2.

Table 2.5.2: Summarized advantages and disadvantages for constant potential and double-step chronoamperometry.

	Advantages	**Disadvantages**
Constant potential	◦ Simple	◦ Inherently non-selective
Double-step	◦ Information about the stability of the system ◦ Increased selectivity	◦ More difficult mathematically

2.5.3 Application of amperometry in neurology

Amperometry provides high enough sensitivity and excellent time-resolution to monitor the neurotransmitter release from individual vesicles and the real-time kinetics of such event. Detecting the exocytotic activity is conducted by placing an electrode held at positive potential against the surface of the cell under examination. The release of the neurotransmitters results in an electrochemical current as oxidation of these substances occurs at the electrode. These amperometric signals can be further analyzed to obtain information about intracellular homeostasis as well as the vesicle release probability. In the following parts of this work the focus is on the application of amperometric devices in detecting neurotransmitters and especially glutamate.

3 Neurotransmitters

Communication between neurons is in most cases a chemical process where species called neurotransmitters are released from vesicles at the presynaptic neuron and detected at the postsynaptic end of the synaptic cleft by specialized receptor molecules. The fusion of vesicles into the neuronal membrane and the release of transmitters is mediated by Ca^{2+} influx arising from action potentials that open the ion channels. The process is called exocytosis and as a result of a burst of neurotransmitters is released into the synapse. The binding of a neurotransmitter at the receptor at the post-synaptic end of the synaptic cleft acts as a trigger and causes the information to proceed through various chemical events (Fig. 3.0.4). [5] [9, p. 52-54]

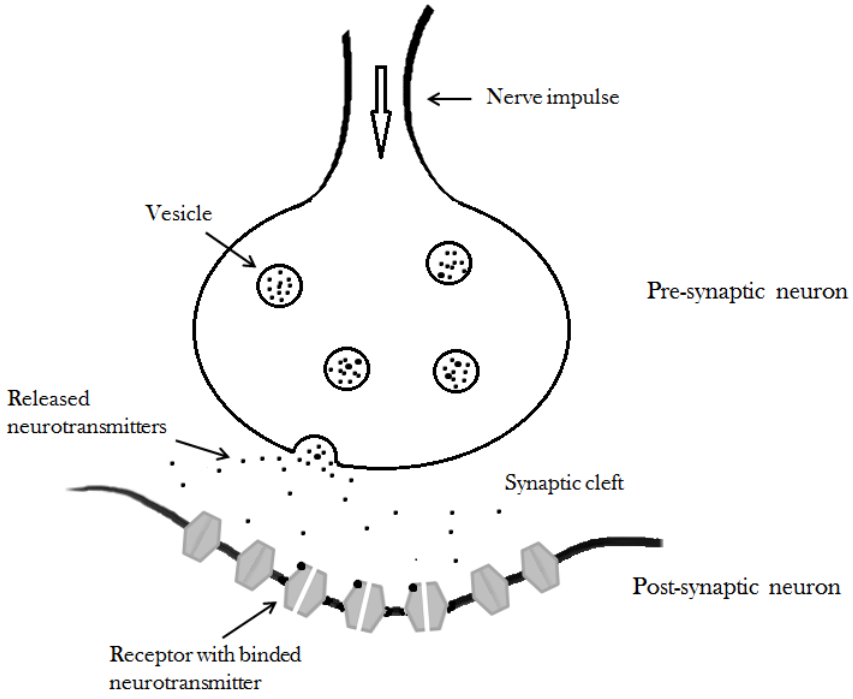

Figure 3.0.4: Neurotransmitter release at the pre-synaptic neuron and binding at receptors located at the post-synaptic neuron causes the flow of information in the nervous system.

Neurotransmitters are the intercellular signal molecules transferring information between neurons in the nervous systems. Small neurotransmitter include such amino acids as glutamate, glycine, and γ-aminobutyric acid (GABA) as well as amines norepinephrine, dopamine, serotonin, and histamine. Larger neuropeptides, which are chains of amino acids, also participate in the signal transfer in the nervous system. In addition, acetylcholine, adenosine triphosphate (ATP), and nitric oxide (NO) have transmitter-like functions. Released neurotransmitters are typically located in the narrow space between two neurons called a synapse but they can also be found in the extracellular fluid. However, in the central nervous system other

types of signalling molecules, hormones for example, exist and distinguishing these from neurotransmitters can be challenging. To make the matter even more complicated, some substances regarded as neurotransmitters have other functions as well: norepinephrine is also a hormone, and both glutamate and glycine are used as building material for proteins. In order to qualify as a neurotransmitter the candidate substance must meet certain criteria [9, p.57].

- First, there has to exist a receptor which activates at the sufficient release of the molecule under examination.
- Second, the substance must be produced by neurons and stored at the nerve terminals from where it is released by calcium dependent depolarization of the plasma membrane.
- Third and final criterion is the existence of an inactivation method for the molecule after its release. Additionally, when the prospective neurotransmitter is artificially applied to the postsynaptic neuron, the results should the same as for the stimulation of presynaptic neuron.

One way to classify neurotransmitters is to separate them into groups of excitatory and inhibitory molecules depending on their effect on the postsynaptic neuron. Also the electroactivity of the molecule can be used as a classification criterion. Some of the most important neurotransmitters with their type as inhibitory or excitatory substance and electroactivity have been summarized in Table 3.0.3. The catecholamines, glutamate, histamine, serotonin, and some of the neuropeptides, to mention a few, are regarded as excitatory neurotransmitters whereas for example GABA, glycine, and some of the peptides inhibit the postsynaptic neuron and are thus regarded as inhibitory substances. In addition, there are also so called conditional neurotransmitters that require the presence of another molecule in the synaptic cleft or activity in the neuronal circuit in order to be effective.

When considering neurotransmitter one important property is their electroactivity since it affects their detectability by, for example, electrochemical methods. Electroactive species, such as dopamine, norepinephrine, and epinephrine, can be directly detected by electrochemical oxidation. Some of the neurotransmitters are not innately electroactive within practical potential ranges. This group involves amino acidic neurotransmitters glutamate, GABA and acetylcholine as well as its precursor choline. Electrochemical detection of these molecules can be conducted by first enzymatically oxidizing the molecule and then measuring the electroactive products, e.g. H_2O_2. In addition to neurotransmitters, other molecules including AA, uric acid, NO, and molecular oxygen can be detected by electrochemical methods. [5] Especially the oxidation of ascorbic and uric acids interferes with the neurotransmitters and thus it is important to find solutions to block these substances from reaching the electrode.

Various psychological illnesses have been suggested to be due to improper functioning of the neurotransmitter system. For example, too high concentrations of dopamine as well as glutamate have been proposed to induce the symptoms of

Table 3.0.3: Some important neurotransmitters with their properties. The electroactivity (+) or electroinactivity (-) is in 0 – 1 V vs. Ag/AgCl.

Group	Substance	Type	Electroactivity	Reference
Amino acids	Glutamate	Excitatory	-	[5, 9, 10]
	Glycine	Inhibitory	-	[5, 9]
	GABA	Inhibitory	-	[5, 9]
Amines	Norepinephrine	Excitatory	+	[5, 9, 10]
	Epinephrine	Excitatory	+	[5, 9, 10]
	Dopamine	Excitatory	+	[5, 9, 10]
	Serotonin	Excitatory	+	[9, 10]
	Histamine	Excitatory	-	[9]
Neuropeptides	Various	Both		[9]
Transmitter-like	Acetylcholine	Both	-	[9, 10]
	ATP	Excitatory	-	[10, 11]
	NO	Inhibitory	+	[10, 12, 13]

schizophrenia. On the other hand, too low serotonin levels are believed to be behind such mental illnesses as depression, anxiety and obsessive-compulsive disorder. In addition to therapy the treatment of these diseases includes the administration of drugs to the patient. These drugs typically either inhibit or enhance the uptake of the neurotransmitter in question. [9, p. 60]

3.1 Glutamate

Glutamic acid, or l-glutamate (see Fig. 3.1.1), is the most abundant neurotransmitter in the brain. It is synthesized either from glutamine by glutaminase in the glial cells or from glucose via the Krebs cycle [5].

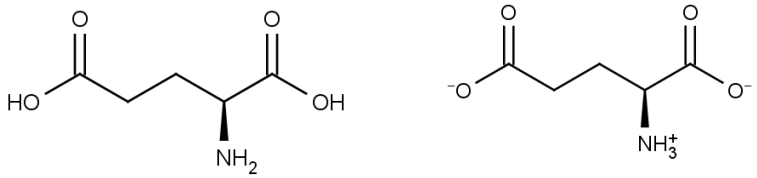

Figure 3.1.1: Structures of l-glutamate (left) and l-glutamate in its deprotonated form in physiological pH (right).

In mammalian central nervous system glutamate acts as the primary excitatory

neurotransmitter. Together with other excitatory amino acidic neurotransmitters it mediates most of the fast and precise synaptic transmission related to perception, movement [14], learning and memory [15]. The excitatory effect arises from glutamate binding with specific receptors. One of these is N-methyl-D-aspartate (NMDA) receptor that allows calsium and other divalent cations to enter the cell. This requires both binding of glutamate and depolarization of the cell membrane. [14] One special feature of the NMDA receptor is its participation in the memory-related phenomenon called long-term potentiation [9, p. 346-347].

Typically, extracellular glutamate levels are in the low micromolar range, whereas the cytosolic concentration are higher, usually in the millimolar range [16]. Transient variations in the concentrations arise from the depolarization of glutamatergic neurons which increases glutamate in the extracellular space.

The functioning of brain neurons at high enough rate requires that the activity of glutamate at the postsynaptic receptors is terminated by its rapid removal from the synaptic cleft [16]. The excess glutamate is normally quickly taken up by astrocytes [16,17] or other transporter molecules [16]. However, when this uptake fails and the brain is exposed to a prolonged high dosage of glutamate it can act as a neurotoxin. As glutamate binding to NMDA together with membrane depolarization allows Ca^{+2} influx into the cell, too high glutamate concentrations have been linked with both apoptotic and necrotic calsium-related cell deaths [18]. For example, during brain hypoxia (lack of oxygen) or ischaemia (stroke) the significant rise in glutamate level can induce serious brain damage [19]. High glutamate levels have been also suggested to be involved in such neurological diseases as schizophrenia [14, 20] and epilepsy [17]. On the other hand, a more recent study by Fayed *et al.* [21] suggest that the glutamate levels in Alzheimer's disease might actually be too low. Moreover, ethanol binding with NMDA receptors, and thus inhibiting the glutamate binding and calsium influx, has related dysfunctioning in glutamate regulation to alcoholism [14].

3.2 Methods to measure neurotransmitters

3.2.1 Microdialysis

Microdialysis is a method where the extracellular fluid of the brain can be probed by using a perfusion fluid that passes through hollow fiber of dialysis membrane. Small molecules, e.g. neurotransmitters, can be analyzed from the dialysate by chromatography and capillary electrophoresis. Electrochemistry and various spectroscopic methods can be utilized for further detection. With the supporting techniques microdialysis is a powerful tool for neurochemical analysis for it offers a high level of sensitivity. [4] However, the relatively large size of the probe can induce tissue damage that has its effect on the measurement. In addition, the size also restricts the spatial resolution, which is typically in the range of 1-4 mm [22]. Furthermore, with microdialysis it is not possible to get real-time information on the release of the particles of interest. [22–24] The temporal resolution can be as low as 30 min which restricts the applicability of this technique in measuring the rapid changes in

the neurotransmitter concentrations [25].

3.2.2 Capillary electroforesis

In capillary electroforesis (CE) a fluid sample is first pulled from the tissue with a vacuum pump through a sampling capillary. By varying the pulling speed it is possible to measure basal levels or monitor the analyte concentrations. After collection the sample is derivatized and injected into separation capillary where the different substances are separated with high voltage. CE can also be combined with for example fluorescense detection. The advantage of CE is the possibility to measure several analytes [24, 26]. In addition, the sample sizes are smalled when compared to microdialysis, which enables sampling at higher frequency and improves the temporal resolution [26]. However, like microdialysis it still lacks the ability to provide real-time data.

3.2.3 Optical methods

Neurotransmitters can be also detected optically. Okubo *et al.* [27] used a hybrid-type indicator that changes its fluorescense upon glutamate binding to it to study extrasynaptic glutamate activity both *in vitro* and *in vivo*. This approach provides a direct method for mapping neuronal structures. A similar examination involving fluorescent indicator molecule was conducted by Hires *et al.* [28]. However, in both of these studies the focus was on the effects of spillover glutamate. Even though the the optical techniques are often coupled with derivatization with the appropriate fluorogenic reagent, it is also possible to detect neurotransmitters without any modifiications for they are weakly fluorescent in nature [29].

Another light-based approach is a method called optogenetics. This technique employs light-sensitive proteins called opsins. In the case of neurotransmitter research opsins are inserted in the brain cells with engineered viruses. After the cell has been "infected" with opsin carrying viruses it is possible to detect its activity by implanted fibreoptic probes. [30] With optogenetics it is possible to measure the neuronal activity of freely moving mammals with good temporal resolution. However, being relatively new technique, there are still many challenges to optogenics, including for example developing light and genetic targeting strategies for different biological systems and animal models. [31]

3.2.4 Biosensors

A biosensor is a device usually containing a biological recognition system, such as an enzyme, whole cells, cell particles or even tissue, for the analyte and a transducer part converting the signal into electrical form [7, 23, 32, 33]. According to this definition not all sensors measuring signals from biological processes can be considered as biosensors. For example, sensors that operate in biological environment measuring pH or oxygen levels but lack the biological recognition element are not biosensors. One important feature of biosensors is that they do not require additional separation procedures or additional hardware or sample processing. By this definition for

example high performance liquid chromatography and flow injection analysis are excluded from the biosensor class. However, both of these methods can include a biosensor as a detector for the analyte. [7] The first biosensors developed by Clark and Lyons [34] in the beginning of the 60's were used to measure oxygen and carbon dioxide levels as well as pH from the blood. The basic principle of immobilizing an enzyme inside a polymer membrane has become a widely used method in the field. However, in 50 years the requirements for biosensors in both temporal and spatial resolution have been lifted to a notably higher scale by the need to detect fast processes from specific areas. Micro or nano scale biosensors offer both spatial and temporal resolution that are high enough for detecting neurotransmitter release in real-time from specific locations thus providing more accurate information about the chemical signalling in the brain compared to for example microdialysis [23, 33].

However, one drawback of the biosensors is that they are typically capable of measuring only one analyte at a time [24]. One option to overcome this problem is to use so called multisite electrodes. In addition to the possibility to measure different analytes simultaneously different geometric electrode configurations enable obtaining information from either smaller brain structures or from larger or layered brain regions. Fig. 3.2.1 presents two possible configurations for four-site microelectrodes. One advantage of the multisite recording is the option to use self-referencing or detect multiple substances simultaneously. Self-referencing electrodes typically include enzyme-free sites that are able to detect all the same substances as the enzyme-coated sites except for the electroinactive species requiring enzymatic degradation. Thus, these so-called sentinel sites collect only the portion of the data provoked by the interfering species, and together with enzyme containing sites provide information about the purely neurotransmitter invoked signal [22].

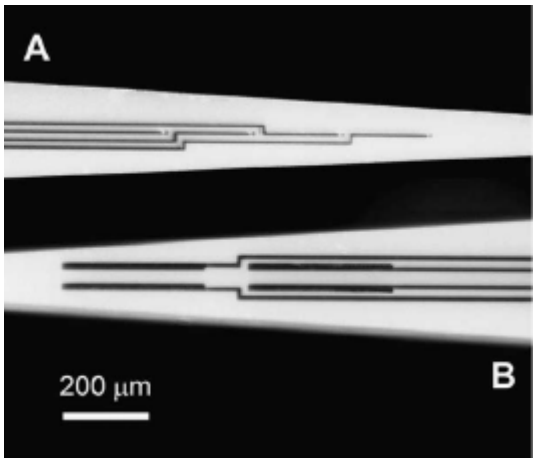

Figure 3.2.1: Two different configurations for ceramic-based multisite recording electrodes. A has four different electrodes in linear arrangement whereas B has two pairs of recording sites. (Modified from [35])

Table 3.2.1 summarizes the different methods for measuring neurotransmitters. Next, the operation of amperometric biosensors in measuring neurotransmitters and espe-

cially glutamate is examined in detail.

Table 3.2.1: Advantages and disadvantages of different methods for measuring neurotransmitters.

	Advantages	**Disadvantages**
Microdialysis	◦ High sensitivity	◦ Tissue damage ◦ Poor spatial and temporal resolution
Capillary electroforesis	◦ Selectivity ◦ Small probe	◦ Low temporal resolution
Optical methods	◦ Good temporal and spatial resolution	◦ Derivatization with fluorogenic reagent or insertion of opsins
Biosensors	◦ Small size ◦ Good spatial and temporal resolution	◦ Selectivity ◦ Bioelement denaturation

4 Biosensors for neurotransmitters

As mentioned earlier, a biosensor is a sensing device containing a biological recognition element. In most biosensors used in measuring neurotransmitters this component is an oxidase enzyme [33]. It is also possible to use dehydrogenase enzymes but this approach is hindered by the required large overpotentials (more than 1 V vs. Ag/AgCl) and the reaction products fouling the electrode surface [36], and thus here we limit the discussion to oxidase enzymes. The enzymatic methods allow detecting non-electroactive species, such as glucose, glutamate, choline, and lactate, electrochemically by immobilizing the enzyme on the electrode. The function of the enzyme is to generate an electrochemically detectable molecule, typically H_2O_2 as shown in equations (33) and (34) [4]:

$$Substrate_R + Enzyme_O \rightarrow Product_O + Enzyme_R \tag{33}$$

$$Enzyme_R + Co\text{–}substrate_O \rightarrow Enzyme_O + Co\text{–}product_R, \tag{34}$$

where R and O refer to the reduced and oxidized forms, respectively. The co–substrate for oxidase enzyme is O_2. For glutamate the reaction with glutamate oxidase enzyme (GluOx) is as follows:

$$Glutamate + GluOx_O \rightarrow \alpha\text{–}ketoglutarate + NH_3 + GluOx_R \tag{35}$$

$$GluOx_R + O_2 \rightarrow GluOx_O + H_2O_2. \tag{36}$$

The H_2O_2 production rate is at the ideal situation directly related to the concentration of glutamate conversed by the enzyme. By immobilizing the enzyme inside a thin film the distance for H_2O_2 to reach the electrode can be made shorter. The H_2O_2 arriving at the electrode is immediately oxidized according to equation (37):

$$H_2O_2 \rightarrow O_2 + 2e^- + 2H^+. \tag{37}$$

In equation (36) the glutamate oxidase uses oxygen as a cofactor to produce hydrogen peroxide. On the other hand, the oxidation of H_2O_2 produces O_2 which enables the continuation of the reaction. However, it is evident that the environment must contain oxygen also in the initial situation in order to oxidize GluOx and generate H_2O_2. [4]

4.1 Sensor materials

The requirements for biosensor materials include in addition to high stability also the ability to resist attack from different biological molecules [37]. Furthermore, the material should of course be electrically conductive. Noble metals, including platinum with its alloys, gold, and palladium, have been experimented as possible candidates [38]. However, metal electrodes such as platinum and gold suffer

from biofouling, and they cannot be used in direct electrochemical detection of neurotransmitters. However, they are commonly used in enzyme based applications where the sensor surface is coated with polymers or other materials. [5]

Various forms of carbon, including graphite, carbon fibres, porous carbon, glassy carbon, and carbon nanotubes, can be used as materials for biosensors [39]. In addition to their cost-effectivity, carbon based electrodes suffer less from biofouling when compared to metal electrodes. Larger potential ranges can also be applied. Especially carbon paste has been widely used owing to its simplicity and low cost [39]. However, even though carbon paste electrodes have good stability *in vivo* the large size limits their applicability [5]. Smaller carbon-based electrodes can be fabricated from **carbon fibres**. The whole size of the electrode can be resticted to micrometer range inflicting less damage to the tissue upon implantation [5]. Carbon nanotubes can also provide some new approaches for enzyme entrapment, electron mediation and nano-biosensor fabrication [39].

4.2 Coatings and enzyme immobilization

According to Qin *et al.* [40] amperometric biosensors can be classified in two generations based on their the redox reactions occurring at the electrode surface and the different electron transfer mechanisms. The so-called first generation sensors use one-step redox reaction catalyzed by oxidase enzyme in the manner previously described by equation (35) and (36). The second generation electrodes, on the other hand, are based on two-step redox reaction. After the enzymatic production of H_2O_2 it is further reduced by a redox mediator, such as horseradish peroxidase or prussian blue. The use of second enzyme allows detecting the analyte at a lower potential to avoid the oxidation of interfering species. In addition to the extra redox reaction the second generation sensors differ from the first generation devices by the physical order of the layers. In the first generations sensors the protection layer blocking the interfering species is deposited under the enzyme layer whereas in the second generation sensors the layers are reversed. A schematic illustration of the two types of sensors is presented in Fig. 4.2.1.

In most biosensors the electrode is separated from the electrolyte by the bioregonition element containing layer. This means that the substrate has to first diffuse into the layer, and after the enzymatic degradation the electroactive species still has to move to the electrode to be detected there. It has been shown that even relatively small deviations in the enzyme layer thickness can result in unpredictable current response [41]. This implies that controlling the thickness of the immobilization matrix should be one of the main concerns when designing enzymatic biosensors. However, the exact control over the layer thickness is seldom achieved, and thus it would be beneficial to develop sensors that are independent from it. Gooding *et al.* [41] showed in their study that changing the electrode geometry so that the substrate must first permeate through the electrode before reacting with the enzyme would result in current response that is not related to the membrane thickness.

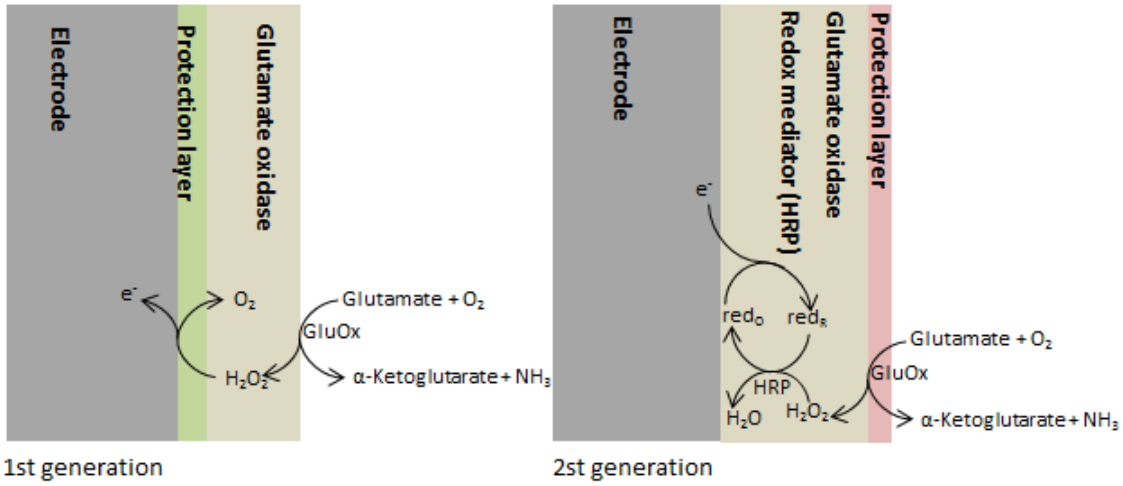

Figure 4.2.1: Schematic illustration of the two generations of sensors. (Modified from [40].)

4.2.1 Enzyme immobilization

The possible deposition methods for the enzyme layer include for example drop coating, dip coating, and spray coating. Qin *et al.* [40] have stated that the needed amount of glutamate oxidase to produce stable sensors is relatively high ranging from 100 to 200 U/mL. However, a study by McMahon *et al.* [42] states that increased enzyme loading on biosensor surface also increases the apparent Michaelis constant, K_M, resulting in poorer sensitivity. This is supposed to arise from increased electrostatic repulsion between anionic glutamate and glutamate oxidase. Optimizing the amount of enzyme is therefore important in regard of sensor performance.

Enzyme immobilization affects various operational factors of the biosensor. The function of these biomolecules is dependent on their structure and the immobilization procedure should not cause any irreversible changes in it. The active site of the enzyme should also be considered. In poorly oriented enzymes the active site may be blocked resulting in partial or total loss of activity. The enzymes should also remain bound to the electrode surface also after immersion in the electrolyte. Thus, it is evident that the immobilization method has to be chosen carefully to obtain optimal stability, sensitivity, selectivity, and response time. In addition the immobilization process should allow good reproducibility. [43]. Fig. 4.2.2 Schematic illustrations of the five most common immobilization techniques.

In **entrapment** enzymes are physically immobilized inside three-dimensional matrices. The matrix can be, for example, electropolymerized film, a photopolymer, silica gel or carbon paste. In this easy method there is no need for modification of the enzyme which enables preserving its activity. Possible disadvantages are, however, escape of the enzyme from the matrix and forming diffusion barriers. Another physical method for enzyme immobilization is **adsorption** which is based on weak van der Waal's forces and electrostatic and/or hydrophofic interactions. A solid support is first placed in enzyme containing solution. After a certain period of

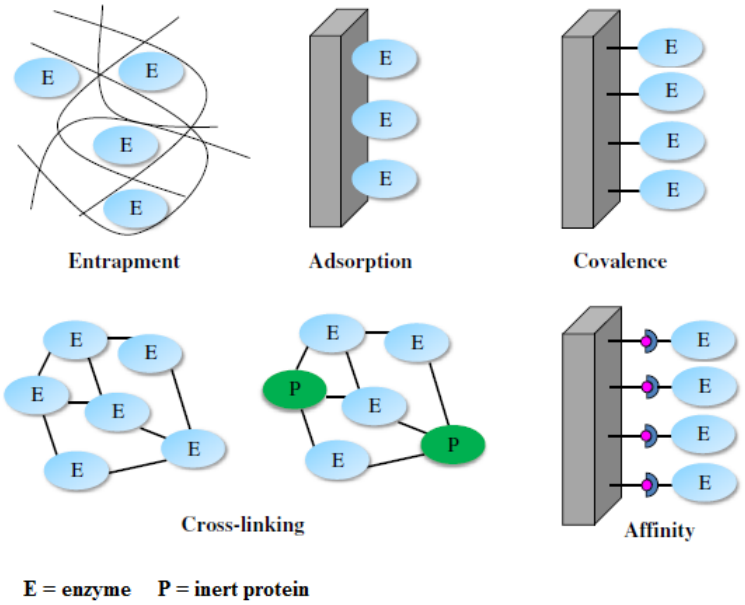

Figure 4.2.2: Schematic illustration of different immobilization methods for enzymes. (Modified from [43].)

time it is removed and the unabsorbed enzyme is washed off. As with entrapment technique, adsorption does not affect the enzyme activity. However, the main disadvantage is the poor operational and storage stability arising from the weak bonds which can easily be broken due to changes in temperature, pH and ionic strength resulting in enzyme desorption. A widely used method in developing biosensors is the **cross-linking** of the enzyme. The cross-linker is typically glutaraldehyde or other bifunctional agent. The enzyme is either cross-linked with each other or functionally inert protein, such as for example bovine serum albumin. The immobilization is chemical in nature which results in strong binding of the enzyme. On the other hand, this type of binding can change the enzyme conformation or chemically alter the active site which both lead to decreased activity. **Covalent coupling** to polymeric supports includes also biocatalysts that are bound to the immobilization surface through their functional groups not essential for their catalytic activity. Multifunctional reagents, such as glutaraldehyde or carbodiimide, are used in the initial activation of the support. After enzyme coupling with the activated support the excess and unbound materials are removed. The enzyme can be either immobilized directly onto the electrode surface or onto a thin membrane fixed on the it. Covalent coupling provides increased stability but the disadvantage of the method is the high amounts of often expensive bioreagent and poor reproducibility. Activated supports are also utilized in **affinity** based immobilization technique. Enzyme binding is site-specific which allows the control of the biomolecule orientation resulting in low deactivation and blocking of the active site. Some enzymes contain the binding-enabling sequence but for others it has to be attached through genetic engineering methods. [43] Table 4.2.1 summarizes the five immobilization methods with their advantages and disadvantages.

Table 4.2.1: Enzyme immobilization methods with their advantages and drawback. (Modified from [43].)

	Advantages	**Disadvantages**
Adsorption	○ Simple and easy ○ Limited loss of enzyme activity	○ Desorption ○ Non-specific adsorption
Covalent coupling	○ No diffusion barrier ○ Stable ○ Short response time	○ Matrix not regenerable ○ Coupling with toxic product ○ High enzyme activity loss
Entrapment	○ No chemical reaction between monomer and the enzyme that could affect the activity ○ Several types of enzymes can be immobilized within the same polymer	○ Diffusion barrier ○ Enzyme leakage ○ High concentrations of monomer and enzyme needed for electropolymerization
Cross-linking	○ Simple	○ High enzyme activity loss
Affinity	○ Controlled and oriented immobilization	○ Need of the presence of specific groups of enzymes

4.3 Biosensor performance criteria

The performance criteria for a biosensor include for example selectivity, appropriate spatial and temporal resolution, sensitivity, and also acceptable limits of detection for each analyte [23]. In addition, also reproducibility, stability and lifetime have to be taken into account when designing biosensors. Thévenot *et al.* [7] suggested in their report four sets of parameters for establishing standard protocols for evaluation of performance criteria of biosensors. The requirements with their respective parameters have been first summarized in Table 4.3.1.

First, the **calibration characteristics** of a biosensor typically include sensitivity, working and linear concentration ranges, as well as detection and quantitative determination limits. In general, calibration can be performed by by adding standard solutions of the analyte and plotting the steady-state responses versus the analyte concentration or its logarithm. The steady state response can be corrected for a blank, i.e. background, signal. Transient responses are generally defined as the maximum rates of variation of the sensor response after the analyte is added in the cell. Usually, the most convenient way to perform the calibration for them is to use a flow system. Transient responses are important for sequential samples but, however, they are less significant when it comes to the continuous monitoring ability of the sensor. By dividing the steady-state or transient calibration curves by the concentrations of the analyte solutions it is possible to obtain the linear ranges and sensitivities in both cases. The upper limit of linear concentration range is directly

Table 4.3.1: Requirements for biosensor performance according to Thévenot *et al.* [7].

Property	Parameters
Calibration characteristics	Sensitivity
	Working and linear concentration ranges
	Determination limits
Selectivity and reliability	Type of sensor
	Response to the analyte
	Response to interfering species
	Reproducibility
Response times	Analyte
	Co-substrate
	Recognition element activity
	Reaction product transport times
Reproducibility, stability and lifetime	Scatter or drift in observations
	Response rate-limiting factor
	Operational conditions
	Storage conditions

related to the biochemical or biological receptor and its biocatalytic or biocomplexing properties. The sensitivity of the biosensor is determined as the slope of the calibration curve from the linear concentration range and it should not be confused with detection limits, which take into account also blank and fluctuation or noise of the signal.

The biosensor **selectivity** depends on the type of the used biosensor. Many enzyme based electrodes are selective towards certain molecules but also class specific electrodes have been developed. Whereas for example oxygen and pH sensors are usually rather selective, metal electrodes are prone to be sensitive to various interfering species as well. The selectivity of the sensor can be determined either by measuring the response for the interfering species and comparing the plotted calibration curve to that of the analyte solution or by detecting the response variation after adding a certain concentration of the interfering substance to the measuring cell containing the analyte solution. The selectivity and the reproducibility together determine the **reliability** of the biosensor. For a reliable biosensor the response is directly correlated to the analyte concentration and it should not vary regardless of the concentrations of the interfering species. The latter requirement includes predetermined toleration limits for interference. [7]

Both the steady-state and transient **response times** depend upon the analyte, co-substrate, activity of the recognition element and product transport times in the bioreseptor immobilization matrix and other layers deposited on the electrode. The properties of these layers, especially thickness and permeability, have have to be

carefully considered when evaluating the biosensor performance. In addition, the mixing conditions can also affect the response time. The hydrodynamic conditions and their effect can be studied by employing a flow system. In *in vivo* applications the transport of analyte and co-substate to the electrode has to be taken into account as well. It is noteworthy that the theoretical modelling of the biosensor operation and performance is often limited by the available information on the properties of the deposited layers and their materials. Determining the thickness of the coating is seldom enough and other parameters, such as the partition and diffusion coefficients and distribution of the biorecognition element, have to be determined for each layer separately in order to fully understand the processes leading to the response.

Reproducibility of a biosensor can be defined as for any analytical device: regardless of place, time or person conducting the experiments within certain limits it has to be possible to obtain similar results without any notable scatter or drift. **Operational stability** of the sensor is especially dependent upon the response rate-limiting factor. In the case of an enzymatic biosensor this can be for example the substrate diffusion to the enzyme in the immobilization matrix or the actual enzymatic reaction. Also the operational conditions such as the analyte concentration, the contact between the sensor and the analyte solution, temperature, pH, and buffer composition, affect the stability. Even though in laboratory conditions some sensors have been reported to operate for periods of one year or longer, the practical **lifetime** of a biosensor can be considerably shorter [7]. One reason for this is the phenomenon called biofouling [33]. Evaluation of the stability and lifetime of a biosensor also includes the determination of proper storage conditions. Important factors include for example the state of the storage, i.e. wet or dry, the atmosphere composition, pH, buffer composition, and presence of additive. [7]

Next, two factors affecting the biosensor performance, interference and biofouling, are examined in more detail.

4.3.1 Interference in amperometric enzymatic biosensors

When measuring enzymatically produced hydrogen peroxide with the biosensor, as often is the case when it comes to neurotransmitters, the needed potential is relatively high, e.g. 0.6 V vs. AgCl/Ag. At this potential various electroactive species found in the brain are oxidized which results as interference in the signal. These interfering species include for example AA, NO, O_2, and H_2O_2. Especially the ascorbate anion has been the the center of attention since it oxidizes at potentials close to dopamine and norepinephrine. It is also one of the most common substances in the brain with concentration range from 200 to 400 μM which gives rise to the need to effectiely prevent it from reacting at the electrode [4].

One option to minimize the effect of the interfering species, such as ascorbic and uric acids, is to use so called self-referencing electrodes. The setup consists of two electrodes placed in each others close proximity by special fabrication methods.The enzymatic coating is deposited on one of the electrodes while the other one has the same coating but without the enzyme. The non-enzyme-containing electrode only detects the interfering species and thus it can be used as a reference for the level

of total interference. The prerequisite is, however, that the chemical environments are equal for both of the electrodes and that the sensitivities for the interfering substances of both electrodes are identical. [5]

Widely used method for the elimination of the interfering species is to use coatings that block these molecules from reaching the electrode. The blocking effect can be based on either the charge of the coating or pore size excluding large particles. Such coatings include poly(o-phenylenediamine) [44] or its isomer poly(m-phenylenediamine) [4], poly(pyrrole) [44, 45], and Nafion® [4]. For example the effect of Nafion® is based on the anionic sulfonic acid groups substituted in the polymer matrix which repel similarly charged particles. On the other hand these negatively charged groups attract cations such as dopamine, catecholamines, and norepinephrine. [4] However, when the molecule of interest is for example glutamate it is important to be able to block previously mentioned substances from the electrode. For this purpose more convenient option is an exclusion layer letting only particles of certain size, for example NO or hydrogen peroxide, pass through. One such coating material is poly(m-phenylenediamine) (pmPD), and in addition to its blocking ability it has three other advantages when compared to Nafion coating. First, the pmPD layer can be deposited on the electrode by electropolymerization after initial coating with the enzyme. This way the matrix forms through the enzyme layer and additional pmPD coatings can be added afterwards without the need to clean the electrode surface. Secondly, electropolymerization enables selective coating of multisite electrodes by connecting only the desired electrodes to the potential source. Finally, unlike Nafion layers, pmPD coatings do not exhibit cracking after soaking and re-drying. [4] Some of the coatings used are summarized in Table 4.3.2.

Table 4.3.2: Different coatings for blocking interfering species in amperometric glutamate sensors.

Coating	**Coating method**	**Reference**
Poly(o-phenylenediamine)		[44]
Poly(m-phenylenediamine)		[4]
Poly(pyrrole)		[44, 45]
Nafion®		[4]

Active removal of interfering AA can also be preformed by co-immobilizing ascorbate oxidase together with the glutamate oxidase [46]. Oxidation of AA at platinum is a quasi-reversible two electron transfer process [47]. The ascorbate oxidase catalyzed oxidation reaction for AA is as depicted in equation (38) [48]:

$$\textit{2-Ascorbic acid} + O_2 \xrightarrow{\textit{Ascorbate oxidase}} \textit{Dehydroascorbic acid} + H_2O. \tag{38}$$

The reaction products are dehydroascorbic acid (DHA) and water. Even though DHA can be easily reduced back to AA, in physiological pH it is quickly hydrolysed to diketogulonate (DKG) [49]. No studies of electroactivity of DKG could be found and it is presumed that it does not further interfere with the electrochemical detection of glutamate. Neither has there been any studies of possible fouling of the

electrode surface by DKG. However, it has been shown that both DHA and DKG are susceptible to oxidation by H_2O_2 [50]. This may have an effect on the operation of amperometric biosensors based on detection of H_2O_2. It is also noteworthy that in physiological conditions AA is not the only interferant for amperometric biosensors. Ernst and Knoll [47] concluded in their article that ascorbic and uric acid can be oxidized simultaneously on platinum surfaces, which should be taken into account in the development of biosensors for neurotransmitter applications.

4.3.2 Biofouling

As any electrical appliance an electrochemical biosensor can suffer from component failures. In addition to the actual electrical failures enzyme degradation and membrane delamination affect the signal. Furthermore, implant materials are exposed to aggressive *in vivo* conditions, and the sensor failure can also result from physiological phenomenon. These physiologically related failure mechanisms include membrane biofouling and biodegradation, electrode passivation, and fibrous encapsulation. In fact, biosensors often perform poorly *in vivo*, which has decreased their commercial potential [51]. Schematic illustration of the different failure types is presented in Fig. 4.3.1.

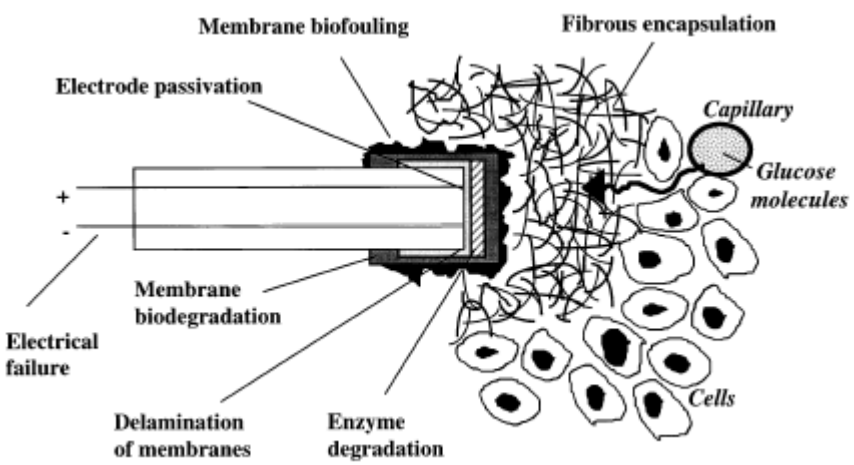

Figure 4.3.1: Schematic illustration for different failure mechanisms of implanted amperometric biosensor containing enzyme encapsulation layer(s). (Modified from [51].)

Biofouling can be characterized as adhesion of proteins and other biological material on the implant surface [51]. Care should be taken not to confuse it with process called electrode fouling, i.e. electrode passivation, that is related to biological substances penetrating the electrode membrane and modify the underlying metal surface. Biofouling, on the other hand, is driven by adsorptive and adhesive interactions of proteins and cells at the sensor surface in contact with tissue [52].

Fibrous tissue encapsulation also affects the implant performance. In sensor applications it restricts the analyte from reaching the electrode, and thus results in decreased signal. The formation of the capsule is similar to scar formation in normal skin wound healing [52], and it is also the final stage of the healing response of the body to the implanted, non-degradable device [53]. Even though biofouling and fibrous tissue encapsulation are clearly two separate phenomena they both result in similar decrease in the sensor response, which makes it difficult to differentiate their effects from each other, especially without *in vitro* calibration [51]. However, one way to separate the two mechanisms is the time scale for their initiation: for biofouling it takes only from minutes to hours for proteins and other substances to adhere to the sensor surface whereas encapsulation requires tissue formation which spans from weeks to months [52].

Wisniewski *et al.* [52] have reviewed different methods for reducing biosensor biofouling. They suggested that biomimicry and perfusion technologies could provide solutions, especially in short-term applications. However, the authors also concluded that none of the methods they reviewed was able to completely eliminate biofouling, which would be desirable for long-term implantable biosensors.

4.4 Production of hydrogen peroxide at enzymatic amperometric biosensors

When the electrochemical reaction is presumed to be diffusion-limited steady-state current i_{SS} at unmodified amperometric disc microbiosensor can be theoretically assumed to be [3, p. 174]

$$i_{SS} = 4nFr_0D_RC_{\infty,R}, \tag{39}$$

where n is the number of electrons transferred, F is the Faraday constant, r_0 is the disk radius, D_R is the diffusivity of the electroactive species R (reduced state) in the electrolyte, and $C_{\infty,R}$ is the bulk concentration of R. However, in enzymatic biosensors the production of the reacting species depends on several factors, including the concentration of the analyte in the bulk solution, on enzyme reaction kinetics, and on mass transport in both polymer and electrolyte solution. Moreover, this affects the net rate of diffusional mass transport of R to the electrode, i.e. the flux of R marked $J_{E,R}$. The resulting current has more complex form compared to the one predicted by equation (39). Hence, more general expression for the current takes the following form:

$$i_{SS} = nFJ_{E,R}. \tag{40}$$

One of the targets in developing amperometric enzymatic sensors for glutamate and other electroinactive species is the production of the often polymeric layers both containing the enzyme and inhibiting the interfering molecules, such as ascorbic and uric acids. As these layers are in many cases custom-made there is no information readily available about, for example, their mass transfer related characteristics. One such characteristic is the diffusivity for the analyte A. In the electrolyte its value

may be well know but in order to construct an analytical model for predicting the current signal the diffusivity in the polymer matrix must be determined. This is often obtained through the partition coefficient which relates the diffusivities of A in both electrolyte and the polymer, and is in fact a property of the system rather than the coating layer alone.

After diffusing into the coating the analyte A is enzymatically degraded into products of which one is typically electroactive and can be electrochemically detected at the underlying electrode. Possible mechanisms for the enzymatic production of the electroactive species R are presented in Table 4.4.1. It is evident that in three out of these four mechanisms increasing bulk concentration of the analyte A, $C_{\infty,A}$, results in higher production rate for R, and thereupon also in an increased response.

Table 4.4.1: Possible mechanisms for for the enzymatic production of the electroactive species R from the analyte A. In the table K_i is the Michaels constant for species i, and V_1 and V_2 are the reaction rates. (Modified from [32].)

	Schematic representation	Source terms
Uni Uni		$S_R = -S_A = \frac{V_{max} C_A}{K_A + C_A}$
Bi Bi	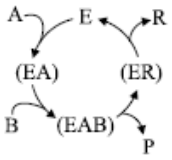	$S_R = -S_A = S_B = V_{max} \frac{C_A C_B}{K_A C_B + K_B C_A + C_A C_B}$
Consecutive Bi Bi	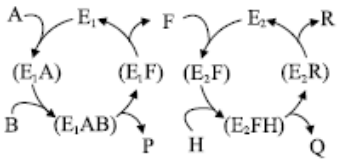	$S_A = S_B = -V_1 \frac{C_A C_B}{K_A C_B + K_B C_A + C_A C_B}$ $S_R = -S_H = V_2 \frac{C_F C_H}{K_F C_H + K_H C_F + C_F C_H}$ $S_F = -S_A - S_R$
Competitive Bi Bi	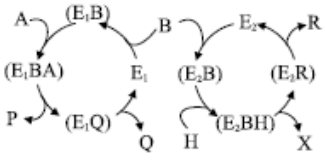	$S_A = -V_1 \frac{C_A C_B}{K_A C_B + K_{B1} C_A + C_A C_B}$ $S_R = V_2 \frac{C_B C_H}{K_{B2} C_H + K_H C_B + C_B C_H}$ $S_B = S_A - S_R$

Table 4.4.1 also presents the so called source terms S_i for different species. For the electroactive R the source term S_R provides information about its enzymatic production rate. S_R links the concentration of the analyte A to the production of R, and thus also to the current response. As shown in Table 4.4.1 there are also situations where the production of R involves other species than A as well. This in

turn affects the source term of R, and the concentrations of all the involved substances have to be taken into consideration. At steady-state all the concentrations, including the concentration of R, can be evaluated by diffusion-reaction equations (see equations from 41 to 49). Considering the electroactive species R, in addition to the source term representing the rate at which R is produced enzymatically, writing these equations also requires such parameters as the diffusivity of R in the electrolyte, D_R, the partition coefficient θ_{R} relating the concentrations of R in the electrolyte and inside the polymer, and the proportionality constant α_{R}, which is defined as the ratio of the diffusivity in the polymer to its diffusivity in the electrolyte. After these parameters have been determined it is possible to write the coupled diffusion-reaction equations with appropriate boundary conditions:

$$D_R \nabla^2 C_R = 0 \tag{41}$$

in the electrolyte and

$$\alpha_R D_R \nabla^2 C_R + S_R = 0 \tag{42}$$

in the polymer. The boundary conditions can be determined from the concentrations of R in the bulk solution (43) and on the electrode surface (44).

$$C_R = C_{\mathrm{inf},R} \tag{43}$$

$$C_R = 0. \tag{44}$$

At the polymer/electrolyte interface the flux of R is continuous (45) whereas there is no flux on insulating surfaces (46).

$$\alpha_R \left(\frac{\partial C_R}{\partial n}\right)_{polymer} = \left(\frac{\partial C_R}{\partial n}\right)_{electrolyte} \tag{45}$$

$$\frac{\partial C_R}{\partial n} = 0 \tag{46}$$

$$\alpha_R = \frac{D_R^{polymer}}{D_R^{electrolyte}}. \tag{47}$$

In addition to the continuity of the flux (45) at the interface under local thermodynamic equilibrium the conditions in the polymer and electrolyte phases can be written as:

$$(C_R)_{polymer} = \theta_R (C_R)_{electrolyte}. \tag{48}$$

Finally, the flux of R to the electrode can be expressed as

$$J_{\mathrm{E,R}} = -\alpha_R D_R \int_{electrode} \frac{\partial C_R}{\partial n} dW. \tag{49}$$

Typically, the steady state current is solved according to equation (40) by numerical analysis. However, numerical simulation, such as finite element or finite difference techniques, often requires special skills which diminishes its applicability. Hence, analytical solutions provide more simple and user-friendly approach. Kottke *et al.* [32] have proposed a model for a closed-form analytical description of the relationship between the steady-state Faradaic current arising from the redox reaction of the electroactive species R on the surface of disk-shaped ultamicroelectrode, and the bulk concentration of the analyte. Their model, however, is limited to electrodes with certain geometry, which restricts its applicability. In addition, they have listed several conditions that have to be satisfied for the model to be effective. Nevertheless, the study of Kottke *et al.* [32] with its implementation in detecting glucose and adenosine triphosphate [54] provides some useful guidelines for the prediction of the steady-state current in amperometric enzymatic UMEs. However, the model is not covered here in detail, and for more accurate overview it is prompted to refer to the original papers [32] and [54].

4.5 Reaction kinetics for hydrogen peroxide oxidation

If both the polymer film deposited on the electrode and the reaction layer, i.e. the enzyme coating, are thin it can be assumed there is no concentration polarization for the analyte inside the film. In this case the steady state response can be expressed as reported by Cooper *et al.* [44]:

$$\frac{i_{SS}}{nWF} = \frac{C_{\infty,A}}{m + cC_{\infty,A}}, \tag{50}$$

where n is the number of electrons transferred, F is the Faraday constant, W is the electrode area, $1/m = \alpha_{loss}\theta_A k_{cat} e_\Sigma l/K_M$ and $1/c = \alpha_{loss} K_{cat} e_\Sigma l/(1+k_{cat}/k\theta_{O_2} C_{\infty,O_2})$. It is noteworthy that both of these are independent of the analyte bulk concentration. In the equations for the constants m and c the coefficients K_M and k_{cat} are the enzyme kinetic parameters for the oxidation of the analyte A (in this case glutamate). The inverse of K_M denotes the affinity of the substrate towards the enzyme. The turnover number k_{cat} can be expressed as the ratio between the maximum reaction rate and the total concentration of the enzyme inside the polymer film, V_{max}/e_Σ. Furthermore, k is the electochemical rate constant for the oxidation of H_2O_2, and l is the thickness of the polymer layer. Finally, θ_{O_2} and θ_A are the partition coefficients for the bulk concentration C_{∞,O_2} of oxygen and the bulk concentration $C_{\infty,A}$ of the analyte. The ratio between the detection of hydrogen peroxide at the electrode and its loss to the bulk solution is described by coefficient α_{loss} [55]:

$$\alpha_{loss} = \frac{1 - D_{H_2O_2,sol} l/2\theta_{H_2O_2} D_{H_2O_2} X_{H_2O_2}}{1 - D_{H_2O_2,sol} l/\theta_{H_2O_2} D_{H_2O_2} X_{H_2O_2}}, \tag{51}$$

where X_D is the diffusion layer thickness and for a microdisc qualifying as an utramicroelectrode it can be replaced by the disc radius r_0, $D_{H_2O_2,sol}$ and $D_{H_2O_2}$ are the diffusion coefficients of H_2O_2 in the solution, and $\theta_{H_2O_2}$ is its partition coefficient in the film. However, this model for the current response is limited to cases where the

polymer layer is very thin. Already in layers that are below 1 µm in thickness the concentration polarization affects the response significantly [56] and the previous equations do not apply for the microcylinder electrode. In this case the current can be approximated according to the model suggested by Somasundrum and Aoki [57]:

$$\frac{i_{SS}}{nF} \approx 2\pi L\theta_A C_{\infty,A} D_A / \ln(\beta), \tag{52}$$

where L is the electrode length, $\theta_A C_{\infty,A}$ is the amount of glutamate inside the polymer film, D_A is the diffusion coefficient of analyte, and β is the ration between the distances of the electrode surface r_0 and the polymer film surface r_1 from the center of the cylinder. In equation (52) it is assumed that the polymer is non-conducting and all H_2O_2 oxidation occurs at the electrode surface. Since the enzyme reaction is very fast, under these conditions the current becomes controlled by the diffusion of glutamate through the polymer film region near the solution interface. In this case the hydrogen peroxide generation also takes place near the surface from where it must diffuse to the electrode according to equation (51). For large values of β, i.e. thick polymer layers, more hydrogen peroxide can escape to the solution resulting in decreased current response [57].

4.5.1 Hydrogen peroxide on platinum surface

The operation of amperometric biosensors is often based on the oxidation of hydrogen peroxide at platinum surfaces. Hall *et al.* [58–62] have made an extensive study on multiple factors affecting this phenomenon with both rotating disk electrodes and microelectrodes. In the first part of their study [58] they proposed a model for the H_2O_2 oxidation by using different H_2O_2 concentrations and electrode rotation rates. It had been previously found out that H_2O_2 oxidation takes place around 600 mV which is the same potential region as for platinum oxide film formation [63], and thus it was presumed that the reaction is favored on oxidized Pt surfaces. It was also noted that there are two inhibiting mechanisms present: the competitive binding of oxygen at platinum and uncompetitive protonation of the platinum/H_2O_2 complex. Both of the inhibiting species are formed as reaction products and in order to reach maximum response and sensitivity their effective removal from the vicinity of the electrode is important. The focus of the second part of the study [59] was on the effect of potential on the oxidation. The authors suggested that near the open circuit potential located at +244 mV vs. Ag/AgCl the reduction of H_2O_2 competes with oxidation resulting in flowing cathodic currents. In addition, it was presumed that between potential range from +244 mV to 600 mV the response arises from the formation of binding sites, i.e. platinum oxides, H_2O_2, and that the reaction becomes fast only at high anodic (E > +600 mV vs. Ag/AgCl) potentials. In the third part [60] Hall *et al.* examined the effect of temperature on H_2O_2 oxidation. The previously developed model for the oxidation mechanism could be successfully applied to explain the temperature dependence of the steady-state responses. Moreover, the nature of the binding sites was further examined and as their number was shown to vary with temperature it was suggested they are formed from precursors

termed Pt_{PS}. However, neither the nature of the precursor nor the binding sites were further determined. Biosensors are usually tested and operated in buffer solutions containing phosphate ions. The fourth part of the study [61] extended the investigation of H_2O_2 oxidation outside the commonly used phosphate concentration and pH. It was revealed that $H_2PO_4^-$ is involved in the formation of the binding site, and thus the number of the binding sites depends on the buffer concentration. This applies at pH $>$ 6.8 but, however, at more acidic conditions the formation of binding sites from precursors is inhibited by protons. Both the phosphate-mediated and phosphate-free mechanisms are presented if Fig. 4.5.1. The upper section presents the H_2O_2 oxidation mechanism that predominates in phosphate-containing electrolytes under physiological conditions. The oxidation of H_2O_2 can also occur in phosphate-free conditions as shown in the lower section of Fig. 4.5.1. However, both of these mechanisms can suffer from inhibition caused by O_2 or protonation. In the phostphate mediated case oxygen binds to the empty binding site and protonation affects the the binding site-H_2O_2 complex. In the phosphate-free mechanism, on the other hand, both forms of inhibition affect the precursor site.

Finally, the formation of the response was summarized as follows [62]:

$$H_2O_2 + Pt_{BS} \overset{K_1}{\leftrightharpoons} Pt_{BS} \cdot H_2O_2 \tag{53a}$$

$$\left.\begin{aligned} Pt_{BS} \cdot H_2O_2 &\overset{k_2}{\rightarrow} Pt + 2H^+ + O_2 \\ Pt &\overset{k_3}{\rightarrow} Pt_{BS} + 2e^- \end{aligned}\right\} \tag{53b}$$

where Pt_{BS} marks the binding sites at platinum surface, K_1 is the adsorption coefficient of H_2O_2 to platinum, and k_2 and k_3 are the rate constants for upper and lower reactions in equation (53b), respectively. In the last part of their study Hall *et al.* [62] aimed to demonstrate the effect of chloride ions on the reactions modeled previously. It was concluded that due to the inhibitive nature of chloride in the oxidation of H_2O_2 it would be beneficial to try to avoid it as far as possible. However, *in vivo* eliminating chloride completely is impossible, which add one more challenge to the development of biosensors for neurotransmitters.

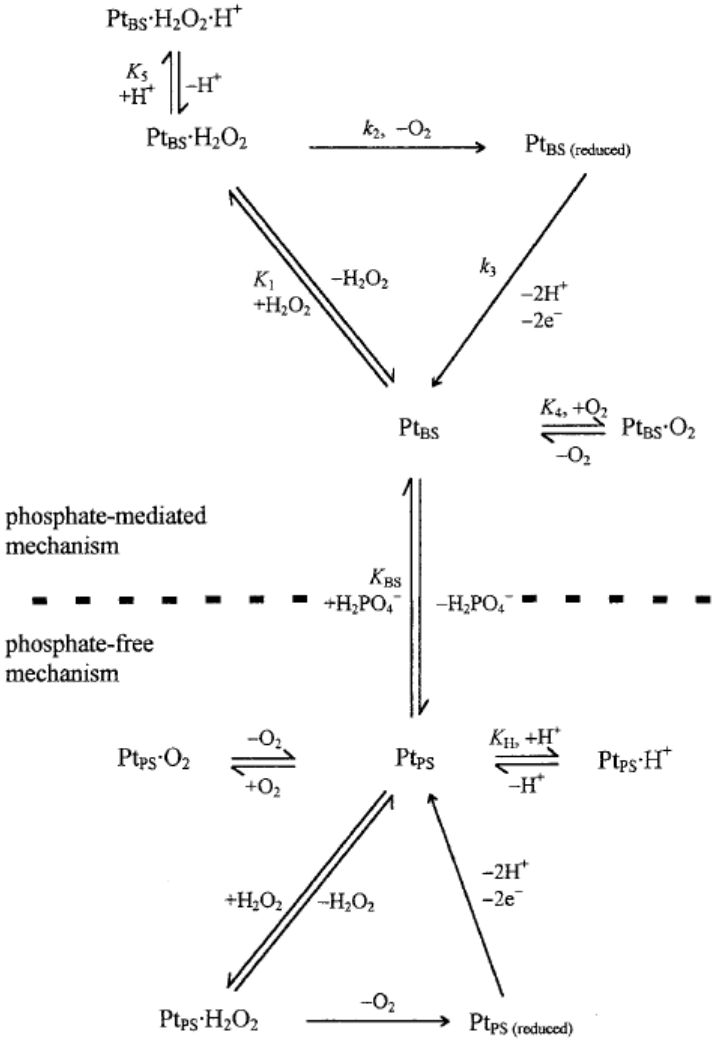

Figure 4.5.1: Phosphate-mediated and phosphate-free mechanisms for the formation of H_2O_2 binding-sites. Here Pt_{PS} denotes the precursor site and Pt_{BS} the actual binding site. (Modified from [61].)

5 Purpose of this work

This work is a part of a strategic opening called ”Carbon based materials in the electrochemical detection of neurotransmitters” in the Department of Electronics in Aalto University. The project aims at development of electrochemical sensors for detection of glutamate and other neurotransmitters. In this work the focus was on detection of glutamate with amperometric biosensors. The aim was to produce and characterize the stuctures of such sensors, and conduct *in vitro* experiments in glutamate and AA containing solutions with them. The effect of temperature was also examined. In addition commercial sensors from Pinnacle Technology Inc. were also used to obtain reference data and verify the applicability of the experimental setup.

6 Materials and methods

6.1 Electrode preparation

The electrodes were prepared from 30 µm diameter platinum/iridium wire (Goodfellow Cambridge Limited, Huntington, England, 90% Pt, 10% Ir) and thin-wall glass capillaries with 1.0 mm diameter (TW100-6, World Precision Instuments, Sarasota, USA). It is noteworthy that as the radius of the Pt/Ir wire was smaller than 25 µm considering the sensors as UMEs was appropriate. The wires were first cleaned by ultrasound bath filled with acetone and dipping them in 40% fluoric acid (Merck, Darmstadt, Germany). As a final cleaning step the wires were etched electrochemically in a supersaturated solution of HCl (J.T. Baker, Avantor Performance Materials, Center Valley, USA) and NaCl (VWR International Oy, Helsinki, Finland). The cleaned wires were fed inside the capillaries and the tips were tightened with a micropipette pulling machine. Next, the capillaries were filled with epoxy (EpoFix, Struers A/S, Ballerup, Denmark), and the protruding Pt/Ir wire was carefully pulled inside to obtain short enough electrode tip. A conducting wire was installed inside the epoxy filled capillary and the electrodes were left to dry overnight. Next day the Pt/Ir wire was soldered onto the conducting wire and the junction was covered with epoxy glue (Loctite Power Epoxy, Henkel Norden Oy, Vantaa, Finland) and two layers of heat-shrinkable tube. Each electrode was tested with multimeter to assure they were operating properly. Finally, the electrode tips were cleaned with acetone.

Before applying the polymer and enzyme-containing layers on the electrode tip they were cleaned in O_2 plasma with plasma cleaner Zepto (Diener electonic GmbH, Ebhausen, Germany). This was done to prevent possible epoxy residues interfering with the coating process. The actual coating with the polymer and enzyme layers was performed in the Department of Biomedical Engineering and Computational Science (BECS) in Aalto University. However, the information about the materials and methods used was unavailable at the time of writing this thesis. A flow chart of the electrode preparation process is presented in Fig. 6.1.1.

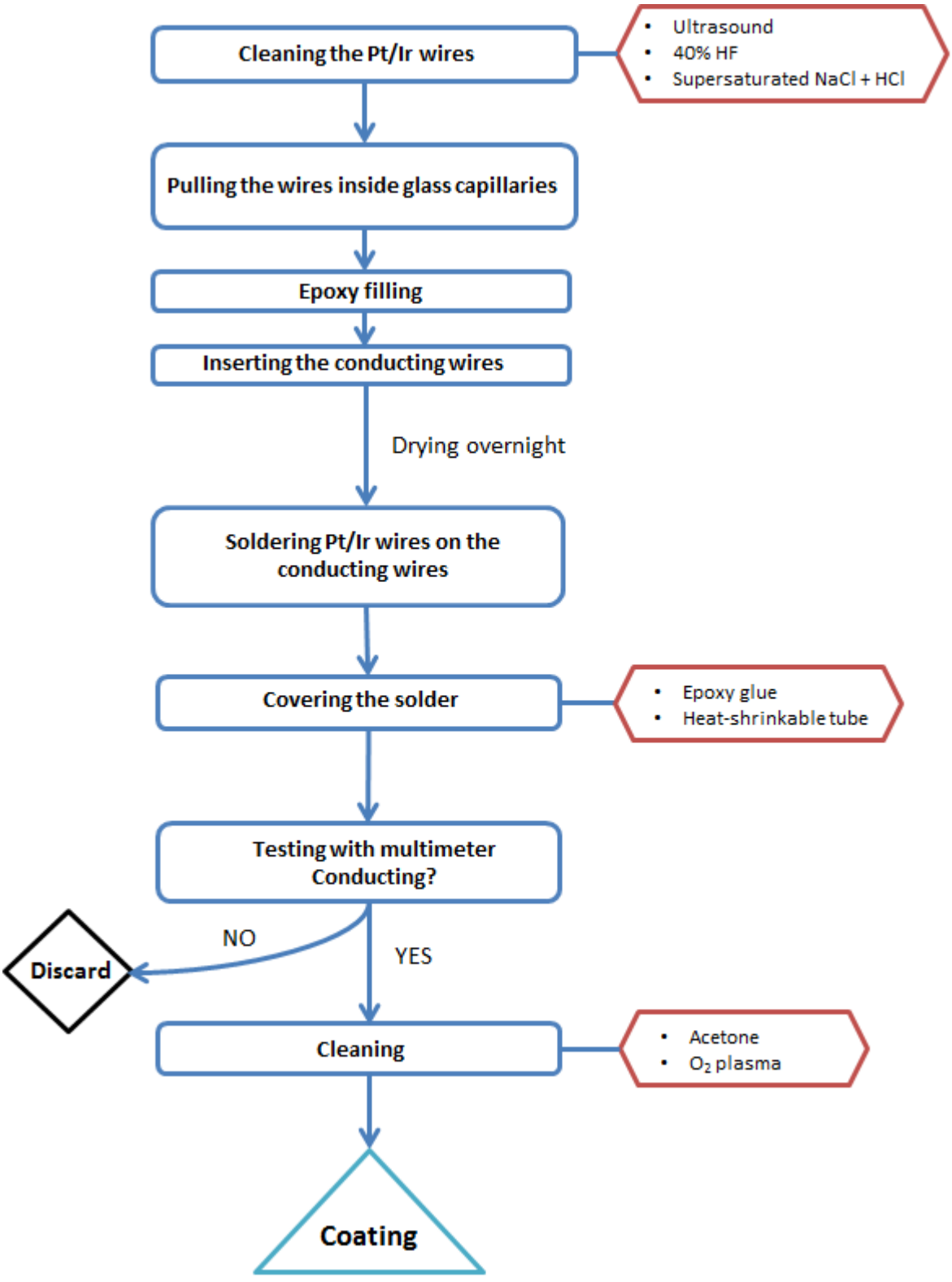

Figure 6.1.1: A flow chart of the electrode preparation process.

Pinnacle sensors

A set of five glutamate biosensors was also ordered from Pinnacle Technology, Inc. (Lawrence, USA). These sensors have been shown to be capable of measuring real-time changes in glutamate levels in the brains of mice and rats for up to 36 hours. The working electrode was a Pt/Ir wire (90% Pt, 10% Ir) with a silver wire wrapped cocentrically around it to function as an integrated Ag/AgCl reference electrode. As the sensor are suitable for *in vivo* there is also an epoxy tip at the end of the electrode to protect it during implantation. The actual sensing cavity between the reference electrode and epoxy covered tip was approximately 1 mm in length. The electrodes were coated with an exclusion layer permitting H_2O_2 pass through but limiting larger and negatively charged molecules from reaching the metal surface. In addition to L-glutamate oxidase the outermost layer contained also L-ascorbate oxidase to further remove interfering AA from the vicinity of the electrode. [46] A schematic illustration of the electrode composition is presented in Fig. 6.1.2. One aim for the use of these commercial sensors was to obtain reference data for further use in electrode development.

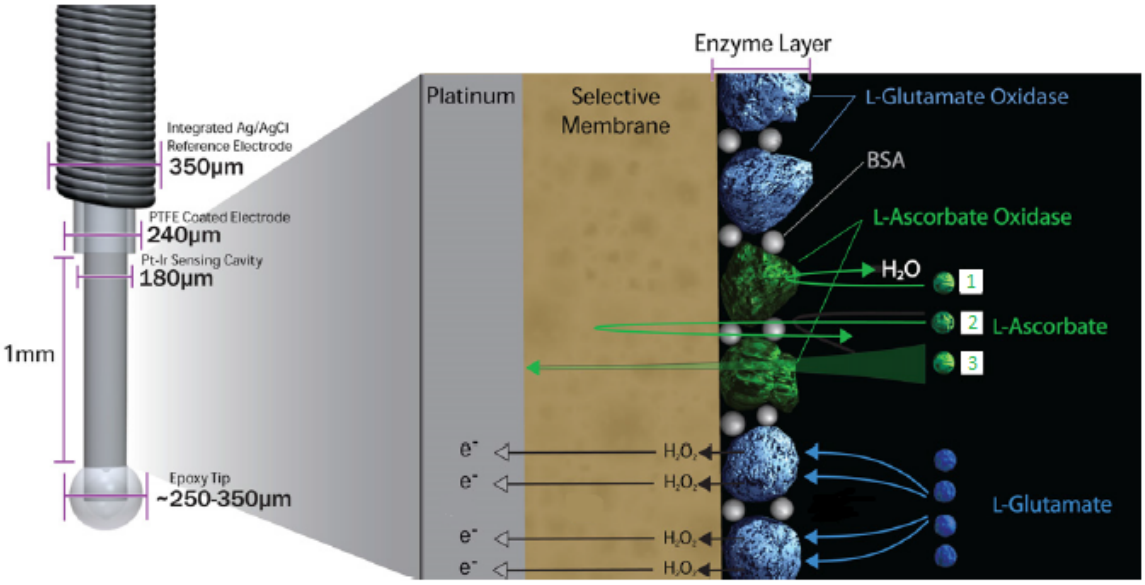

Figure 6.1.2: Schematic illustration of the L-glutamate sensors ordered from Pinnacle Technology, Inc. These sensors apply two different mechanisms for the removal of interfering L-ascorbic acid: a) L-ascorbate oxidase immobilized in the enzyme layer converts ascorbic acid into electroinactive dehydroascorbate and water (box 1), and b) the inner semi-permeable layer limits large and negatively charged molecules from reaching the electrode surface (box 2). Some of the ascorbic acid, however, can reach the electrode but this amount is sufficiently small not to affect the signal (box 3). (Modified from [46].)

Two sensors were used to measure glutamate and two in AA experiments. One electrode was saved for later use.

6.2 Imaging

In order to get more information on the layers deposited on Pt/Ir surfaces the electrodes were observed both under optical microscope (Olympus BX51M, Olympus Co., Tokyo, Japan) and in scanning electron microscope (SEM) (JSM6330F, JEOL Ltd., Tokyo, Japan). Optical microscopy did not affect the electrodes so they could be observed both before and after experiments. The electrodes were inspected before and after the polymer/enzyme coating. The lengths of the Pt/Ir wires protruding form the capillary tip were measured with the imaging software (The Leica Application Suite, Leica Microsystems, Wetzlar, Germany) from the pictures taken before coating.

For SEM imaging the electrodes were coated with chromium with a sputtering device (Emitech K575X, Quorum Technologies Ltd., Ashford, USA) to avoid charging of the non-conducting parts. As the chromium coating would destroy the electrodes SEM imaging was not performed on the Pinnacle sensors before the experiments. In order to obtain some information of the structure of the coatings on these sensors two sensors from previously ordered set were examined in SEM.

6.3 Electrochemical measurements

The sensitivity experiment were conducted in phosphate-buffered saline (PBS) with pH 7.4 – 7.6 in a glass beaker at both room temperature and 37 °C (see Fig 6.3.1). PBS was either purchased from Biochrom AG or prepared in the laboratory according to Table 6.3.1. 10 mM glutamate and AA stock solutions were prepared by dissolving 0.368 g of L-glutamic acid powder (Sigma Aldrich, St. Louis, USA) in 250 ml PBS and 0.176 g of L-ascorbic acid (Sigma Aldrich) in 100 ml PBS, respectively. Glutamate stock solutions were divided into 10 ml aliquots which were stored in freezer and thawed no longer than 5 days before experiments. For AA is easily oxidized by air stock solutions were always prepared on the day of the experiments. Experiments were conducted in different concentrations of glutamate (both sensor types) and AA (Pinnacle sensors only) shown in Table 6.3.2. Pinnacle Technology Inc. gives the detection limit of 0.05 – 0.1 µM for their sensors, and the lower glutamate concentration limit (0.1 µM) was decided according to this information. On the other hand the information that glutamate levels in the extracellular space are in the micromolar range was used to determine the upper concentration limit. For the self-made electrodes only five different concentrations were used (0 µM, 0.1 µM, 1 µM, 10 µM, 100 µM). However, for Pinnacle sensors it was decided to include also concentrations of 50 µM and 200 µM in order to be consistent with previous experiments [64] with commercial electrodes. In order to avoid electrical interference the beaker and the electrodes were placed inside Faraday cage (VistaShield, Gamry Instruments, Warminster, USA). For the self-made electrodes a separate Ag/AgCl reference electrode was also connected to the potentiostat. Between the

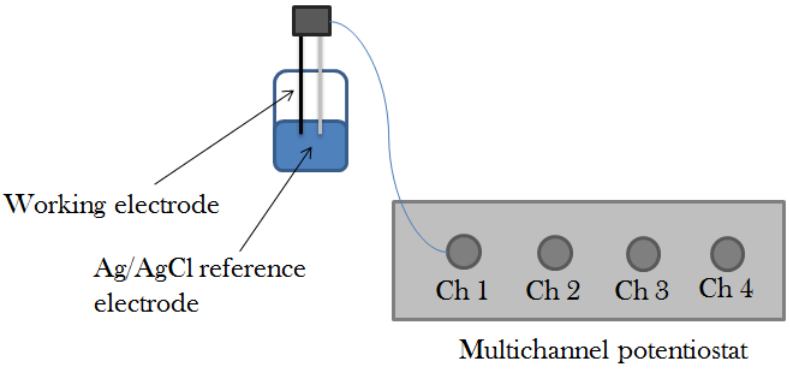

Figure 6.3.1: Schematic illustration of setup for sensitivity experiments. The potentiostat (here channel 1) was used to both control the sensor potential and collect the resulting current response. Note that for Pinnacle sensor with integrated Ag/AgCl electrode no separate reference electrode was needed.

Table 6.3.1: Dissolving the ingredients in 1000 ml of DI-water gives 1 litre of 10x PBS stock solution. The PBS used in the experiments was further diluted by adding 9 litres of DI-water.

Ingredient	Mass (g)
NaCl	80.0
KCl	2.0
Na_2HPO_4	14.4
KH_2PO_4	2.4

Table 6.3.2: Experimental conditions for both glutamate and AA experiments.

	Concentrations (µM)	Baseline (mV)	Step (mV)
Glutamate	0, 0.1, 1, 10, 50, 100, 200	200	620, 420
Ascorbic acid	100, 500, 70, 1000	0	620

experiments conducted on different weeks the sensors were stored in dry conditions at room temperature.

Glutamate experiments

During the experiments the electrodes were first immersed in the solutions for two minutes at 200 mV baseline potential. This baseline value was decided upon the result by Hall *et al.*. They proposed that when measuring hydrogen peroxide oxidation on platinum surfaces negative currents are measured in more lower potentials than +232 mV [59]. After two minutes the potential was stepped in anodic direction for 10 seconds and then returned back to the baseline level. For self-made electrodes the potential step was 620 mV and for Pinnacle sensors 420 mV (see Table 6.3.2). In addition, for some of the self-made electrodes the potential was stepped momentarily to -400 mV between the measurements in different concentrations. This was though to purge the electrode vicinity from possible reaction products. However, the nature and actual existence of these supposed products was not examined further, and thus it was considered more appropriate to conduct the experiments without the extra voltage step.

Ascorbic acid experiments

In AA experiments the electrodes were similarly first immersed in the solutions for two minutes at certain baseline potential and after that a potential step was applied on them. However, for AA the oxidation potential on platinum surfaces is 200 mV, and thus a baseline potential of 0 V instead of 200 mV had to be used. The potential step was done to 620 mV similarly as in the glutamate experiments with Pinnacle sensors. Even though this voltage is clearly higher than the AA oxidation potential it was assumed that using the same potentials as for glutamate would benefit more to the future work where the aim is to simultaneously measure the sensitivity and selectivity.

6.4 Flow chamber

The temporal resolution of the sensors was examined with a previously designed flow chamber system. The advantage of this type of equipment is that it enables moving the electrode from the buffer solution to the analyte containing solution without removing it from the solution environment. The liquid flow in the flow channel was achieved by a syphon system. The sensor was connected to the active holder element which could be set between the "up" (sensor in the buffer solution) and "down" (sensor in the glutamate solution) positions through control potential of 1.5 V automatically fed from a multichannel potentiostat. Due to the total size of the equipment the flow chamber experiments could not be performed in Faraday cage which might have increased the electrical interference in the signal. In addition, the current system only allowed performing the experiments in room temperature solutions. Schematic illustration of the flow cell system is presented in Fig. 6.4.1. More detailed description can be found from the previous work by Olli Kotiranta [64].

Mixing of the analyte solution flowing in the channel and the buffer solution was

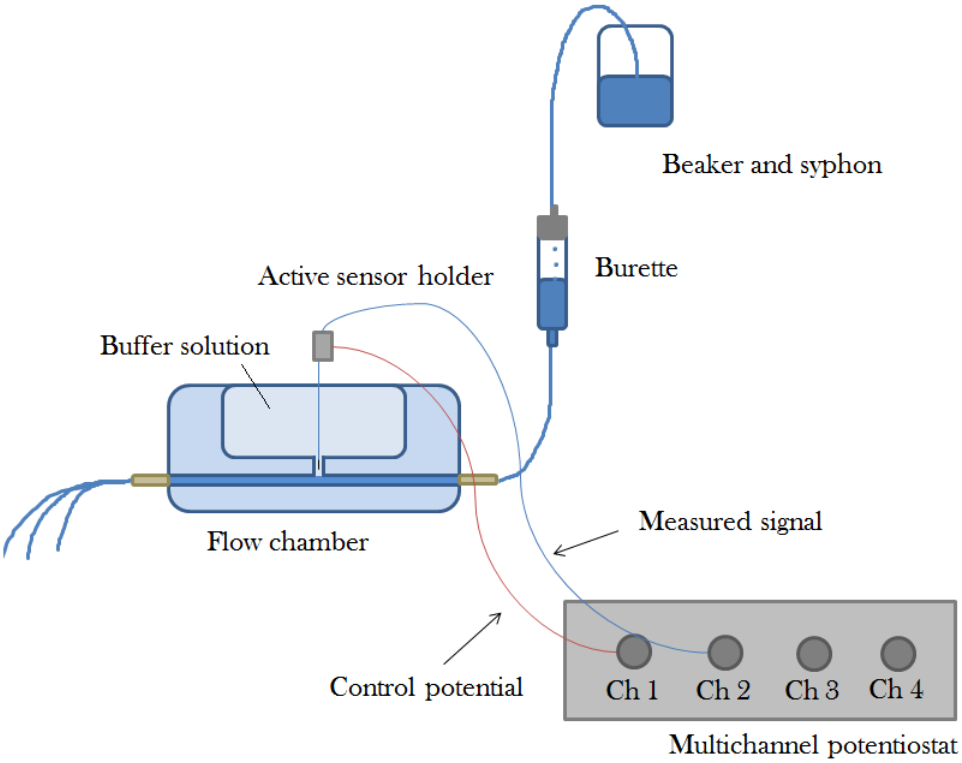

Figure 6.4.1: Schematic illustration of the flow chamber system. The sensor is in the "up" position. Channel 1 (red chord) controls the sensor holder potential and the sensor position. Channel 2 (blue chord) is used to both control the sensor potential and collect the resulting current response.

avoided by adjusting the liquid pressure. This was done by balancing the outflow rate with the filling speed of the burette. The electrode was first carefully placed in the connection channel between the buffer solution containing reservoir and the flow channel. After two minutes immersion the electrode was dipped into the liquid flow for 6 seconds and then pulled back to the connection channel for four seconds. The dipping was performed eight times in a row. During the experiment the electrode was kept at 620 mV vs. Ag/AgCl. The potential was switched off while the analyte solution was changed but electrode was not removed from the buffer solution once it had been immersed.

6.5 Potentiostat and data analysis

The potential between the working and reference electrodes was controlled with a potentiostat (e-corder 821, eDAQ, Denistone East, Australia). The potentiostat was operated through Chart^{TM} software (ADInstruments Pty Ltd, Colorado Springs, USA). Chart^{TM} was also used for recording the data from the electrode. In the flow chamber experiments Chart was also utilized simultaneously feed the control voltage

to the active sensor holder.

Data analysis was performed with MATLAB® (MathWorks, Natick, USA). In order to be able to compare the data measured with different sensors the current response was first divided by the area of the electrode to get the current density on the electrode surface. Next, three and half seconds worth of the current density from the end of the 10 seconds voltage step were averaged. The error was obtained as standard deviation of the current density in this region. Finally the averaged values for all the concentrations were plotted together.

7 Results and Discussion

The electrodes were structurally characterized by optical microscope and SEM imaging. The response of self-made and commercial amperometric glutamate sensors to different concentrations of glutamate and AA in PBS was observed with two different methods. The sensitivity analysis was performed by placing the electrodes in and open beaker. The experiments were repeated in two different temperatures, room temperature and 37 °C. The temporal resolution was observed with a custom made flow system in room temperature only. The results are presented next.

7.1 Electrode characteristics

The average length of the electrode tip was 0.96 ± 0.29 mm (n = 20). The large deviation in the tip lengths was explained by the sensors being prepared one by one and controlling the exact length was difficult.

From the optical microscope images it was also observed that on some electrode surfaces there were some residues from the electrode fabrication process (Fig. 7.1.1). These residues were presumed to be epoxy and as it might affect the polymer coating by changing the wettability of the surface the electrodes were cleaned with oxygen plasma before coating.

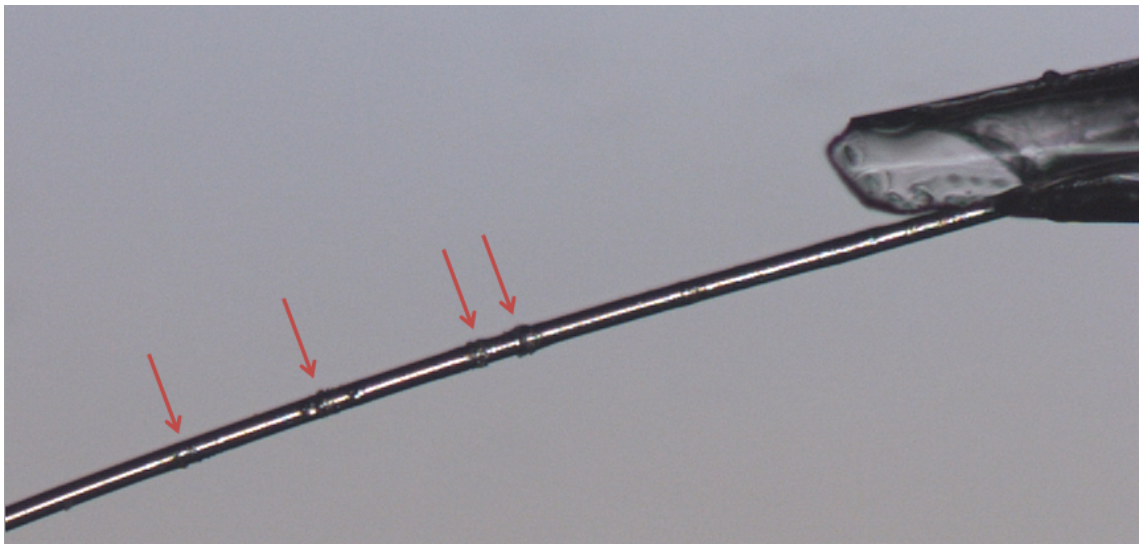

Figure 7.1.1: Optical microscope image of a self-made sensor with visible epoxy residues. The red arrows mark the residues on the the platinum wire surface.

The cleaning effect of O_2 plasma was verified by dipping a piece of the platinum wire in epoxy. After drying the epoxy could be clearly seen on the wire. After the plasma treatment the epoxy had been completely cleaned. The same wire before and after plasma treatment is presented in Fig. 7.1.2. In normal electrode preparation process the epoxy residues were significantly smaller, and thus O_2 should also remove them.

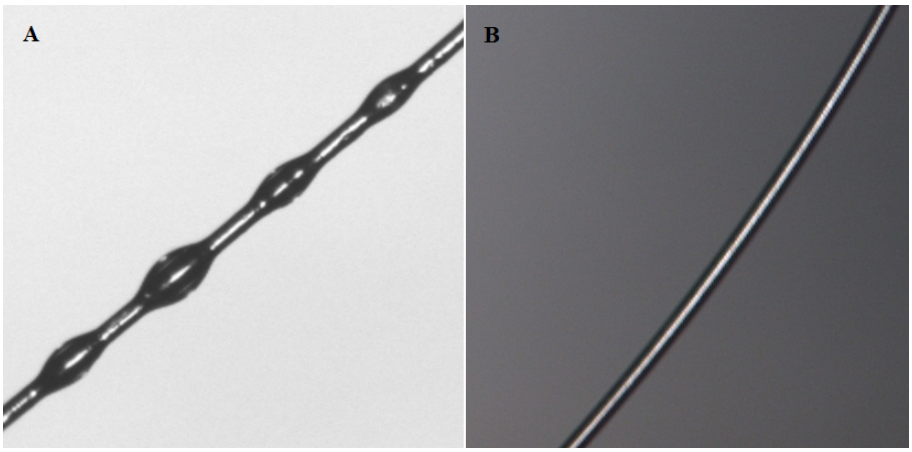

Figure 7.1.2: Optical microscope images of platinum wire dipped in epoxy before (A) and after (B) treatment with O_2 plasma.

Examining the self-made sensors after coating under optical microscope revealed that no significant changes could be observed with this method (Fig. 7.1.3). It was presumed that more detailed information could be obtained by SEM.

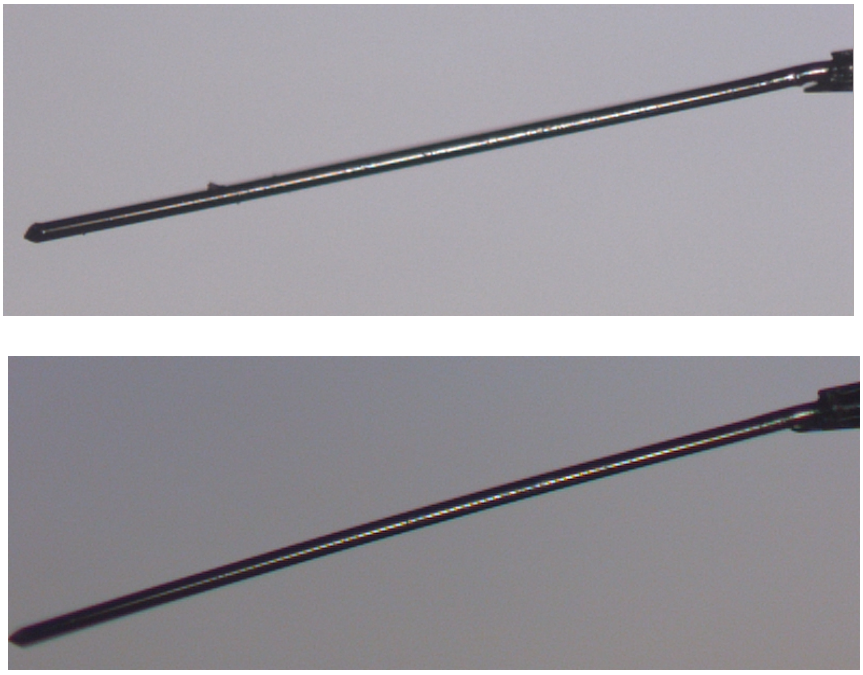

Figure 7.1.3: Optical microscope image of the electrode before (upper) and after (lower) polymer/enzyme coating.

An important aspect of the self-made sensor characteristics was the variation in the quality of the coatings. Figure 7.1.4 presents a SEM image of an sensor only coated with the polymer exhibiting fairly smooth surface structure. However, in

some cases adding the enzyme layer changed the surface morphology significantly as shown in Fig. 7.1.5. Such large accumulations of the enzyme solution were also visible on the optical microscope and sensors exhibiting this type of structure were not used in the experiments.

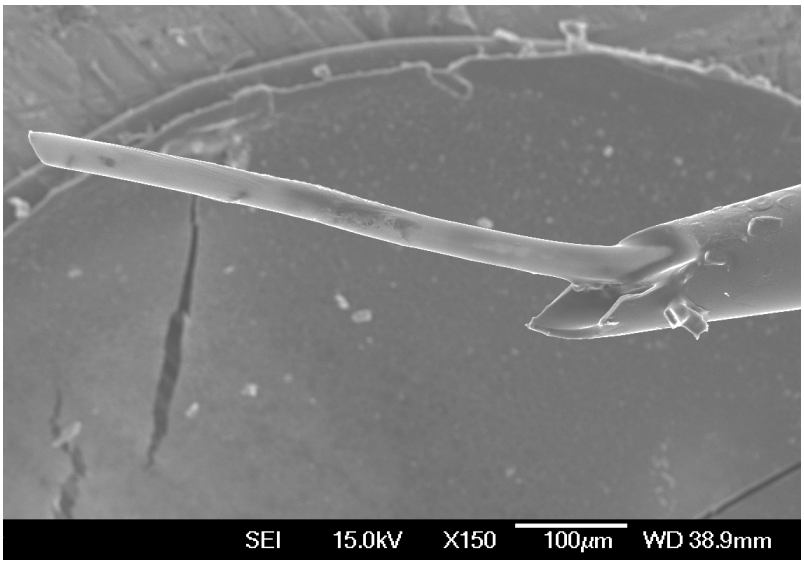

Figure 7.1.4: SEM image of the polymer coated self-made sensor before experiments.

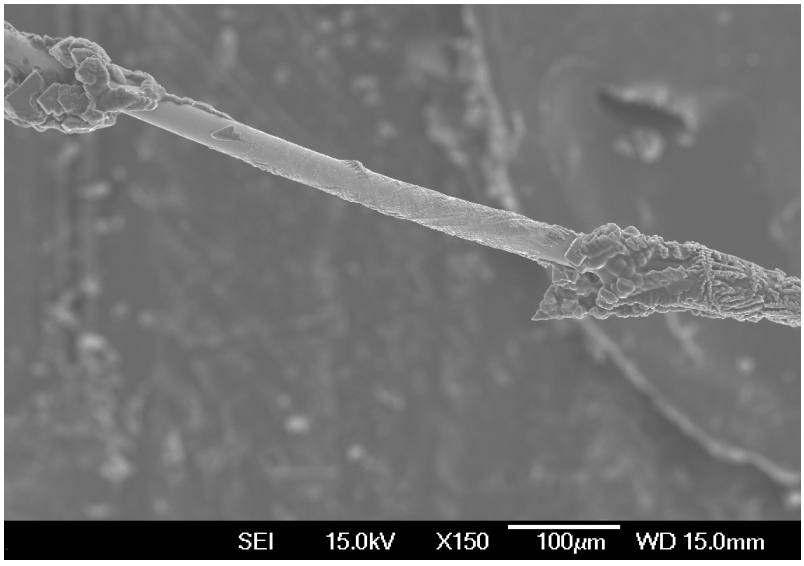

Figure 7.1.5: SEM image of the both polymer and enzyme coated self-made sensor before experiments.

On the other hand it was also possible that the coating was peeled off from the electrode surface during the experiments. In Fig. 7.1.6 the red arrows point

out the spots where the platinum surface has been exposed. This indicates that the adhesion between platinum and the coating material was not adequate. Qin *et al.* [40] stated that after successful enzyme coating a thin yellow transparent layer should be visible on the electrode surface under optical microscope. However, no such layers were detected on the sensors utilized in this work. This is proposed to arise from the non-uniformity and possible poor adhesion of the coatings. It is suspected that there was never a continuous and uniform coating on the surfaces of self-made sensors which should be considered when examining the results from the experiments.

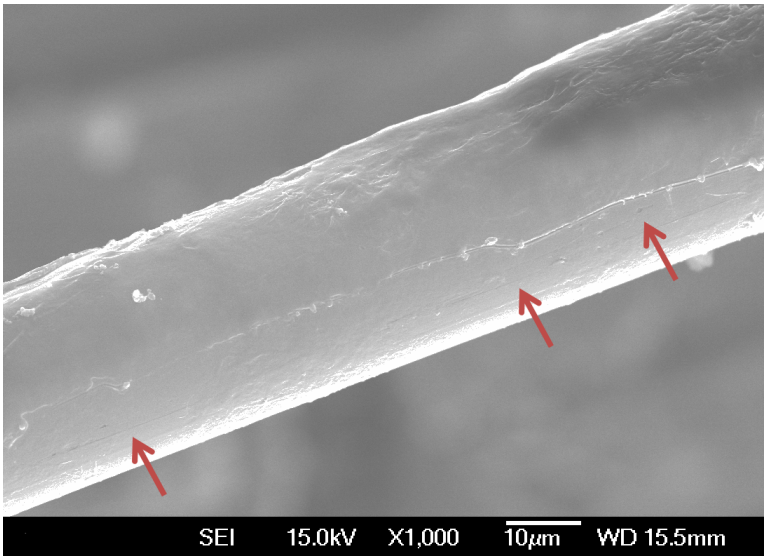

Figure 7.1.6: SEM image of a polymer and enzyme coated self-made sensor after experiments. The red arrows point out the marks on the platinum surface indicating that the coating has been peeled off.

Pinnacle sensors were only examined under optical microscope. Fig. 7.1.7 shows one of the sensors on the day of the experiments and another a week later. The sensor was stored in dry at room temperature. It is visible even from the optical microscope images that the sensor coating has been damaged during the storing period. It is proposed that the coating first absorbed liquid when immersed in the buffer solution. During drying this liquid evaporated resulting in cracking of the coating layers. Pinnacle Technology Inc. does not recommend reusing the sensors after drying which is possibly due to uncertainty in the results arising from the cracking [65].

7.2 Sensitivity

Self-made sensors

The sensitivity experiments to glutamate were conducted by placing the sensor in a 30 ml beaker filled with the analyte solution. After two minutes immersion a

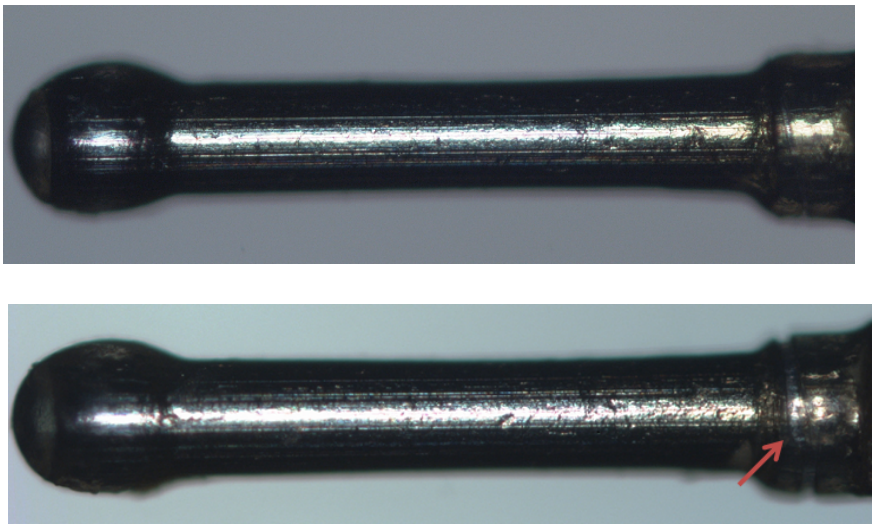

Figure 7.1.7: Optical microscope image of one of the Pinnacle sensors before immersion in the solutions (upper) and after drying and storing in dry room temperature conditions for one week (lower). The red arrow marks the crack formed on the coating layer during the storing.

potential step was applied on the electrode. The resulting current density was as shown in Fig. 7.2.1. The averaged current densities both at room temperature and at 37 °C for one of the self-made electrodes from experiments conducted within a four weeks period are presented in Fig. 7.2.2.

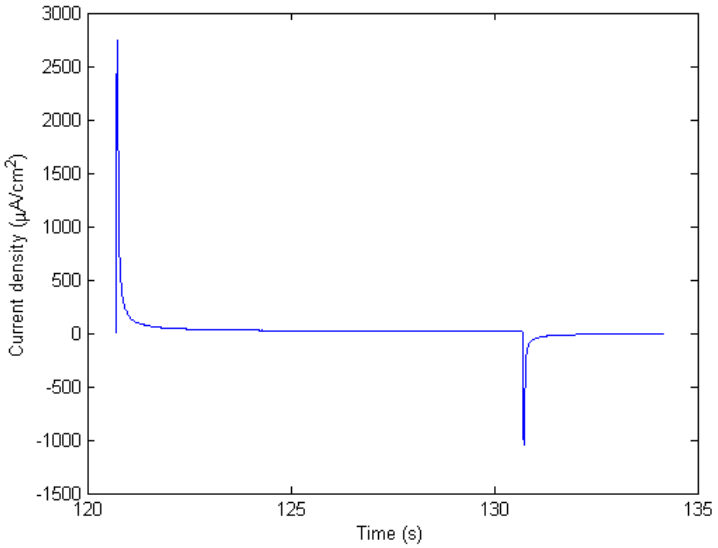

Figure 7.2.1: An example of the resulting current density from the experiments conducted in the beaker with enzyme coated self-made sensor.

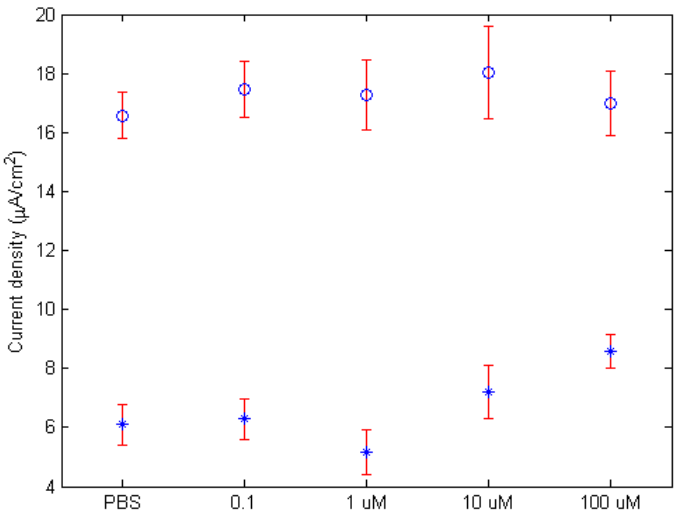

(a) Week 1

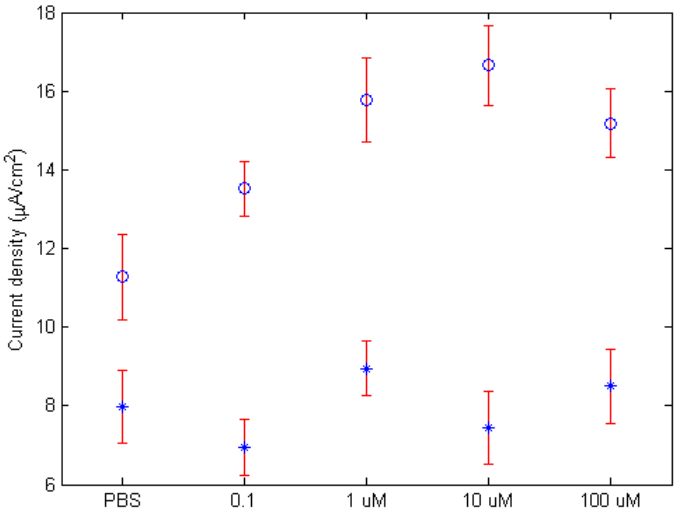

(b) Week 2

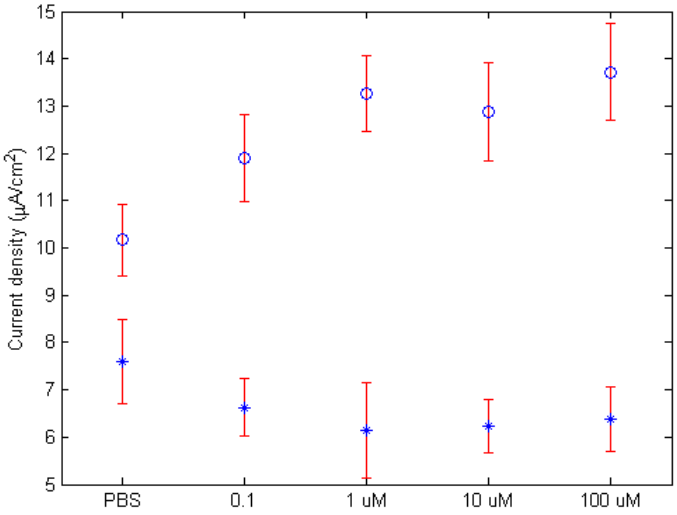

(c) Week 4

Figure 7.2.2: Averaged current density responses for glutamate in 37 °C (circles) and in room temperature (asterisks) on weeks 1, 2 and 4 for a self-made enzyme coated electrode.

Interestingly, in all of the experiments the averaged current densities were lower for the room temperature than the 37 °C solutions. As there was no constant heating for the solution the temperature might have decreased during the approximately two and half minutes experiment. The temperature did not, however, drop to the room temperature level during the experiment which supports reliability of the results. On the other hand, similar experiments were also conducted with polymer coated electrodes without the enzyme and pure platinum electrodes. The results showed similar dependence on the temperature of the analyte solution (Fig. 7.2.3).

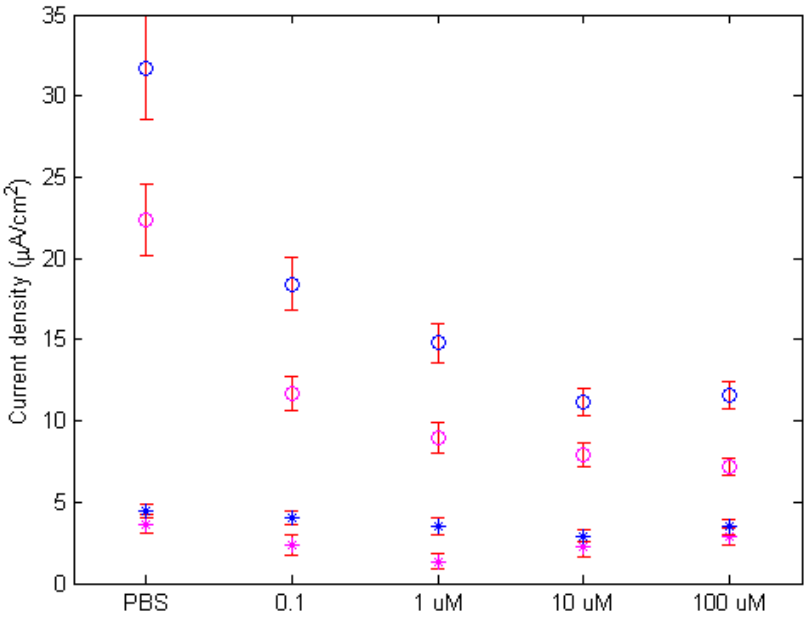

Figure 7.2.3: The current response for glutamate on polymer coated (magenta) and pure platinum (blue) self-made sensors in 37 °C (circles) and in room temperature (asterisks) without stepping the voltage to -400 mV between the measurements. Also these types of sensors exhibited similar temperature depence as did the enzyme coated sensors.

An interesting aspect in the results was the effect of stepping the voltage to the negative direction. This was first done after each measurement to purge possible substances remaining in the vicinity of the electrode. It was, however, difficult to verify the existence and nature of these species and it was considered the best not to perform the additional voltage step. This resulted in the current response clearly decreasing with increasing concentrations in consecutive measurements with the same electrode, which is the complete opposite of the expected behavior. As similar results were obtained for pure platinum electrode it was suspected the self-made electrodes might not be properly coated and the underlaying platinum surfaces were at least partly exposed (see Fig. 7.1.6). The results for glutamate on self-made

enzyme coated biosensor and pure platinum electrode in 37 °C without the additional step to -400 mV between measurements are presented in Fig. 7.2.4.

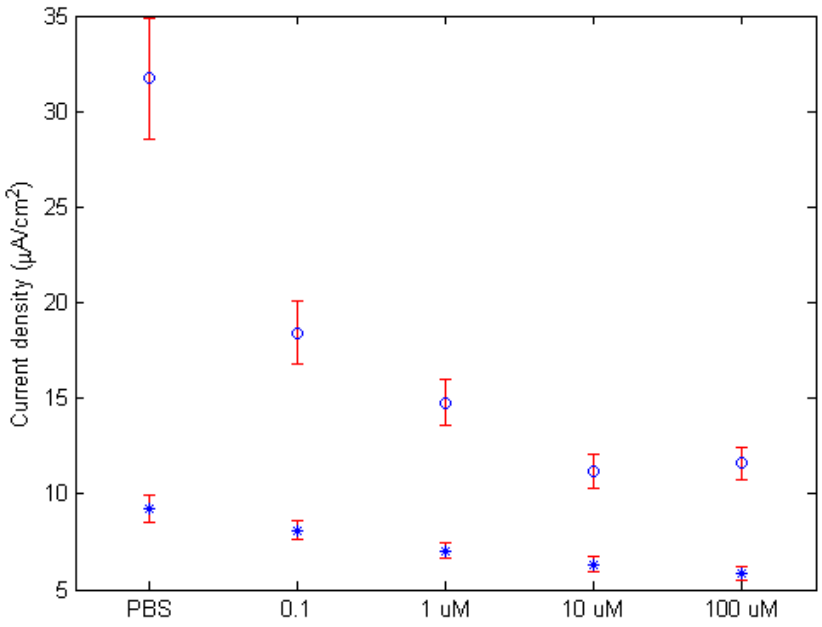

Figure 7.2.4: The current response for glutamate on self-made enzyme coated biosensor(asterisks) and pure platinum electrode (circles) in 37 °C without the additional step to -400 mV between measurements.

Glutamate is not innately electroactive so the response of a pure platinum electrode should not in any case vary with changing the analyte concentration. One possible explanation for the obtained results could be that some other species in the electrolyte solution are oxidizing/reducing on the platinum surface. On the other hand, the increase in glutamate concentration does not affect the concentrations of other substances to such extent that it would have such a significant effect on the results.

The formation of PtO and PtO_2 oxides on platinum surfaces occurs at the same potential region as hydrogen peroxide oxidation [63]. In addition H_2O_2 oxidation is favored on oxidized surfaces [61]. It has been proposed by Hickling and Wilson [66] that the current interpreted as oxidation current of hydrogen peroxide arises actually from the re-oxidation of H_2O_2 reduced Pt surfaces. Adding the results by Yang and Denuault [67] which state that the platinum oxide reduction is a two-step process occurring below -200 mV (vs. custom-made $Hg|Hs_2SO_4|K_2SO_{4(sat)}$ reference electrode) would suggest that the current measured is in fact the oxidation current for platinum. The potential step to -400 mV acts to reduce the oxides formed on the platinum surface. Stepping to potential to anodic direction results in re-formation of these oxides. The voltammogram for platinum measured in PBS presented in Fig. 7.2.5 further supports this.

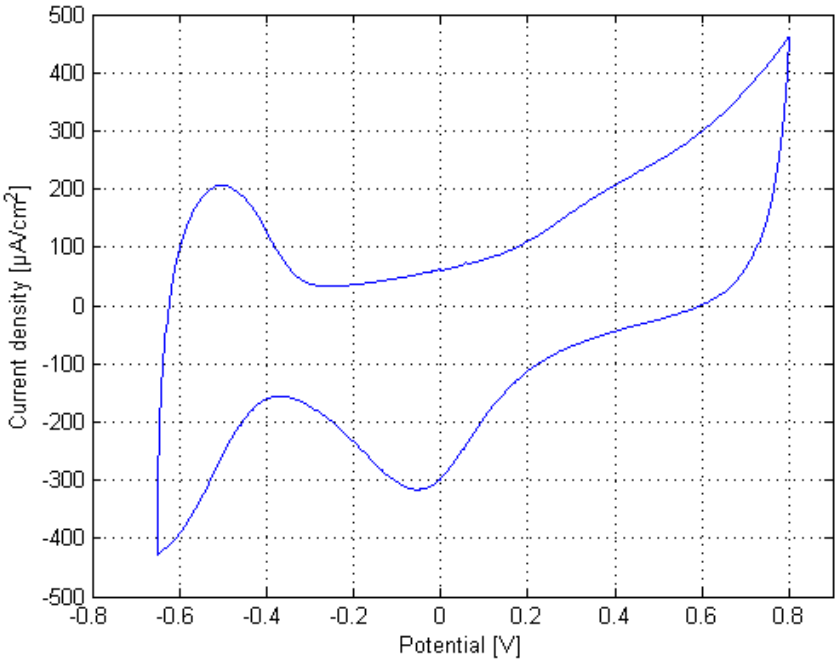

Figure 7.2.5: Voltammogram for pure platinum in PBS.

From Fig. 7.2.5 it can be seen that the formation of platinum oxides (and hydroxides) commences at approximately at 200 mV, and the electrochemical window in PBS is reached at 800 mV. On the other hand, the reduction of platinum oxides begins at approximately 0 mV.

This could explain the decreasing response for the experiments where no cathodic step between the measurements was used (Fig. 7.2.4). After each measurement there was less free places for platinum oxide formation and the resulting current was lower than previously. In addition to the surface of the enzyme-containing sensor being possibly partly coated these sensors were also pre-treated with oxygen plasma whereas the pure platinum electrode was not further cleaned after preparation. This could also explain the higher response for the pure platinum sensor. In Figures 7.2.2b and 7.2.2c the responses measured in 37 °C are increasing with increasing concentration. Further investigation is, however, out of the scope of this work.

Pinnacle sensors

Similar experiments were also conducted with commercial sensors that have been verified to produce appropriate response to glutamate solutions. Pinnacle was chosen as the provider according to adequate results in our earlier intial experiments with their sensors (results not reported). However, the Pinnacle sensors used here have been optimized to work *in vivo*. As it is very challenging to model the physi-

ological environment in a beaker the results obtained here might not represent the true characteristics of the sensors.

The current responses for a Pinnacle sensor in both room temperature and 37 °C are presented in Fig. 7.2.6. Note that also concentrations of 50 µM and 200 µM were included in order to be able to compare the results with earlier results obtained with the flow cell system. Pinnacle has reported a limit of detection for their glutamate sensor to be 0.05 – 0.1 µM However, as seen from Fig. 7.2.6 higher results than that for PBS are obtained only at concentrations higher than 50 µM.

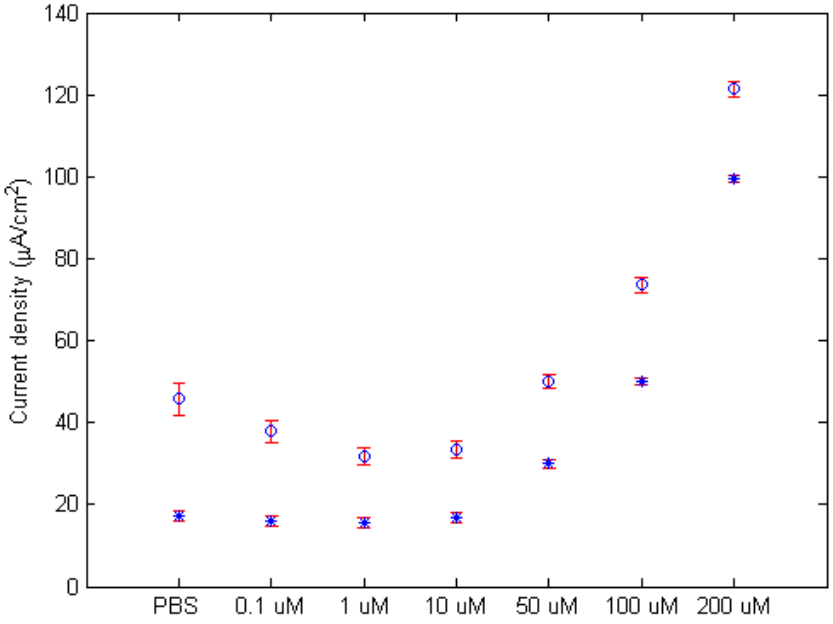

Figure 7.2.6: Averaged current density response for glutamate in 37 °C (circles) and in room temperature (asterisks) for a Pinnacle sensor.

The values for the current density responses on the Pinnacle sensor in solutions containing more than 10 µM have been collected in Table 7.2.1 with calculated ratios for the current density responses in different temperatures. According to Wachiratianchai *et al.* [68] the relative activity of glutamate oxidase drops from the maximum at approximately 37 °C to 60% at room temperature. It is suggested that similar ratio should be observed also in the current density response since the current response should be proportional to the enzymatically produced H_2O_2, and thus also dependent on the enzymatic activity. However, as seen from the data presented in Table 7.2.1 the proposition is incorrect as the ratios of the current densities at different temperatures are increasing with increasing concentrations. This is possibly a result from the enzymatic production rate for hydrogen peroxide with increasing bulk concentration of glutamate as proposed by Kottke *et al.* [32] (see also Table 4.4.1).

One important performance criterion for biosensors is their ability to produce a

Table 7.2.1: Averaged current density responses with different concentrations of glutamate in 37 °C and room temperature (RT) with their respective ratios for a Pinnacle sensor.

Concentrations (µM)	Current density (µA/cm^2) (37 °C)	Current density (µA/cm^2) (RT)	Ratio (%)
50	50.1	30.0	60
100	73.6	50.1	68
200	121.3	99.4	82

linear response in their operational range. Pinnacle reports that their biosensors are capable of operating linearly at least to concentrations of 50 µM. Fig. 7.2.7 shows the data obtained with Pinnacle sensor with an included linear fit.

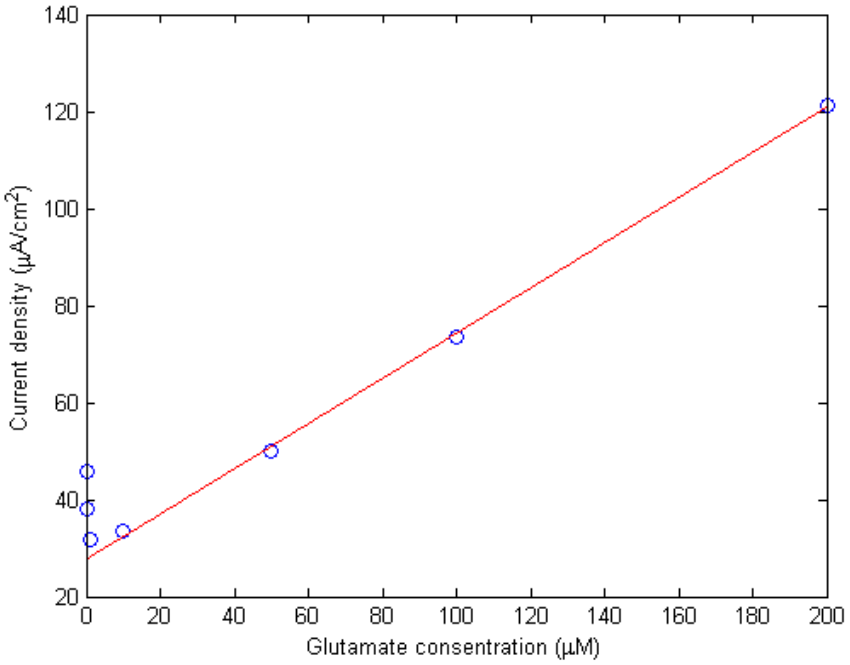

Figure 7.2.7: Linear response for the Pinnacle sensor measured in 37 °C. The slope is 0.5 µA/cm^2/µM and the respective R^2 value 0.99.

However, as already discussed the response for the lowest concentrations differs significantly from the expected behavior. Hence, concentrations lower than 10 µM have been excluded from the fitting. Typically, the linearity is expressed as the slope of the fitting curve. For the data presented in Fig. 7.2.7 the slope is 0.5 µA/cm^2/µM and the respective R^2 value representing how appropriate the fit is. The closer R^2 is to one, the better the fit.

The first glutamate experiments with self-made sensors were conducted with a

voltage step of 620mV. In these experiments the baseline potential of 200 mV was not considered thus resulting in higher final potential (820 mV) than initially planned. The oxidation potential for hydrogen peroxide is 600 mV vs. Ag/AgCl, and this value is typically used when measuring glutamate amperometrically. Also Pinnacle recommends this voltage for their sensors. However, there have been studies where amperometric glutamate experiments have been carried out at 850 mV vs. Ag/AgCl [44], which would support the assumption that this potential is equally applicable. On the other hand Hall *et al.* set their upper limit at 712 mV vs. Ag/AgCl in their study of hydrogen peroxide oxidation at platinum surfaces stating that higher potentials would suffer from competitive oxidation of the buffer solution. However, at this time it remains unclear whether the competition with the oxidising species in the buffer would be a problem also in electrodes coated with layers fabricated from different materials. In order to follow the original plan and recommendations from Pinnacle the experiments with commercial sensors were conducted with a voltage step of 420 mV resulting in final potential of 620 mV. This is believed to be more beneficial also in regard of future research.

7.3 Temporal resolution

The temporal resolution of the sensors was examined using a flow cell previously designed in our laboratory. Typically, the response time of the sensors is defines as the rise time between 10% and 90% of the maximum response. The self-made sensors did not produce any reliable response in the flow cell experiments. Thus, no data for them is presented here. The flow cell system had been previously utilized by Olli Kotiranta to collect data with Pinnacle sensors. A typical current density response is presented in Fig. 7.3.1.

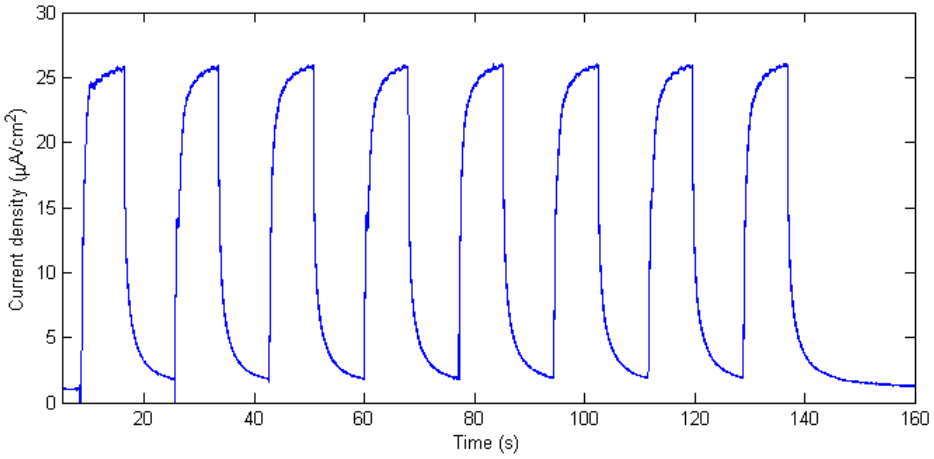

Figure 7.3.1: Current density response for a typical flow cell experiment measured with a Pinnacle sensors. The sensor was dipped in the flowing analyte solution (50 microM) for approximately 8 seconds eight times in a row.

It was possible to obtain a significant response with concentrations higher than 10 µM. In order to compare these results with the ones from previously described sensitivity experiments conducted in the beaker the maximum responses for each experiment were averaged. The results are presented both in Fig. 7.3.2 and Table 7.3.1. Fig. 7.3.2 includes also the linear fit of the data set with slope of 0.3 $\mu A/cm^2/\mu M$ and R^2 value of 0.99. The standard deviations were calculated to represent the error but they are not included in the linearity plot. The flow cell experiments were conducted in room temperature solutions, which is proposed to explain the decrease in the linear response of the sensor compared to the slope of 0.5 $\mu A/cm^2/\mu M$ measured at 37 °C in a beaker.

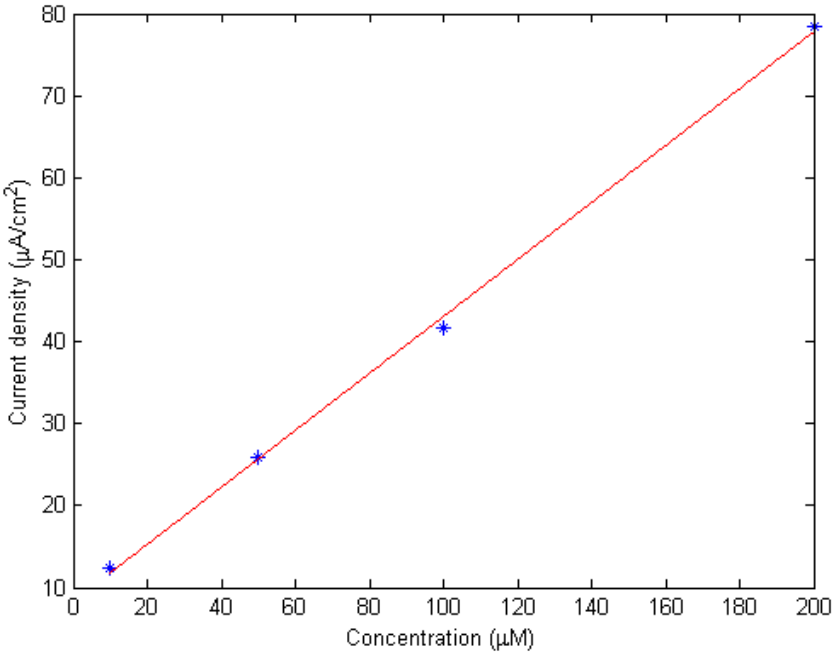

Figure 7.3.2: Linear response for the Pinnacle sensor measured in the flow cell system in room temperature. The slope is 0.3 $\mu A/cm^2/\mu M$ and the respective R^2 value 0.99.

The averaged response times for the four different concentrations are also presented in Table 7.3.1.

7.4 Selectivity

AA is one of the main interfering species for amperometric biosensors. The ability to block this substance can be induced for example by semipermeable negatively charged exclusion layers or by deposition of ascorbate oxidase enzyme on the electrode surface to degrade AA into electroinactive species. However, the self-made sensors had been earlier evaluated as unreliable in the glutamate experiments, and thus the AA measurements could not be performed with them. Pinnacle reports to have chosen to combine both of these approaches on their sensors. The results for

Table 7.3.1: Averaged current densities and response times with their respective standard deviations measured in four different concentration at room temperature for a Pinnacle sensor.

Concentrations (μM)	Averaged current density (μA/cm^2)	Averaged response time (s)
10	11.1±0.2	2.2±0.3
50	24.9±0.5	2.0±0.3
100	40.4±0.1	1.9±0.1
200	77.6±0.1	1.6±0.1

measurements in four different concentrations of AA in 37 °C are presented in Fig. 7.4.1.

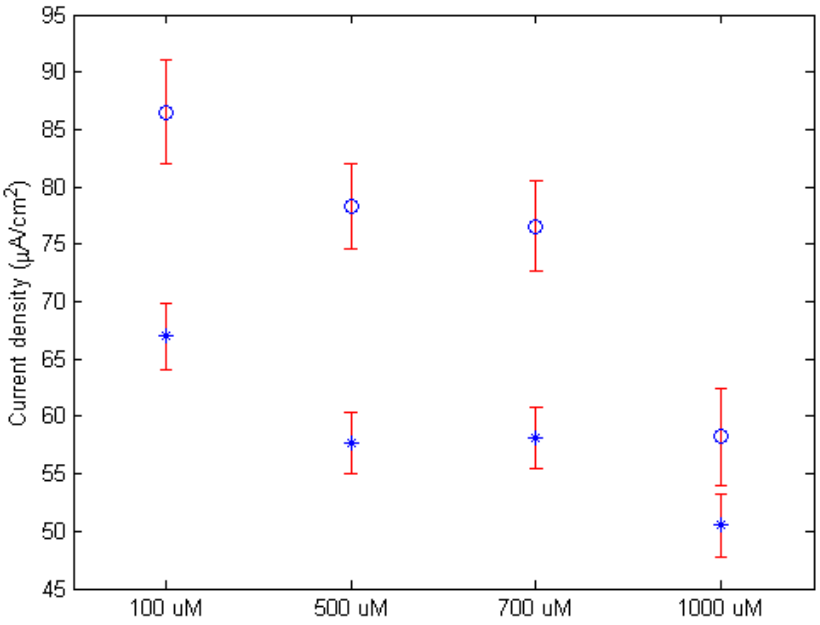

Figure 7.4.1: Averaged current density response for AA in 37 °C (circles) and in room temperature (asterisks) for a Pinnacle sensor.

For a sensor blocking AA effectively the response resulting from measurements with different concentrations of AA should be approximately a straight line. On the other hand, sensor failing at the blocking of the interfering species should exhibit an increasing response as more AA can reach the underlaying platinum surface. However, Fig. 7.4.1 shows that the response for AA is decreasing as the concentration is increased in both 37 °C and in room temperature. One possible explanation for this kind of behavior is the fouling of the sensors surface with reaction products from the AA oxidation.

7.5 Future work

In the future the experimental setup for the sensitivity analysis should be reconsidered. In various studies the analyte concentration is increased by injections of concentrated solution. The voltage is typically held at single potential throughout the whole experiment. For the resulting stepwise response graph it is possible to determine both the linear range and the temporal resolution of the sensor. In addition, the selectivity towards different analytes could also be tested simultaneously. This type of experiment could also easily be conducted in a water-jacketed vessel where the temperature of the solution could be held constant. However, in order to obtain homogeneous concentration after injections the solution has to be constantly stirred.

In addition to the changes in the experimental setup it would be beneficial to explore other methods to detect glutamate than the polymer coated biosensors. Initial experiments with immobilizing enzymes on self-assembled monolayers have been conducted in our laboratory, and they seem to provide an interesting option for the polymeric coatings (not reported yet).

8 Conclusions

In this work the theory and operation of amperometric biosensors were inspected both via literature review and empirical approach. The results have been presented and discussed in the previous chapters with appropriate suggestions for future experiments.

The results from both scanning electron microscopy and electrochemical experiments indicate that the polymer and enzyme layers deposited on the platinum electrode surfaces may not have been uniform. In addition, the coatings were easily peeled off form the electrodes. It is proposed that this results in the main response arising from the oxidation of platinum instead of hydrogen peroxide.

Commercial sensors were bought from Pinnacle Technology Inc. and similar experiments with the self-made ones were conducted with them. It was, however, later acknowledged that these sensors have been optimized for *in vivo* conditions, which explains the unexpected results. Nevertheless, the Pinnacle sensors gave stronger response than the self-made sensors to all concentrations of glutamate. This is considered to further support the assumption that the self-made sensors had not been properly coated.

It was also shown that temperature affects the response on amperometric biosensors. According to previous research this was first suggested to arise from improved enzyme activity in 37 ° solutions compared to room temperature solutions. This was, however, found to be the case also for pure platinum sensors without any enzyme coatings. This indicates that there might have been regions that had not been coated properly on the enzyme surfaces. Hence, improving the coating procedure should be one of the main concerns in future research.

Various aspects in the electrode behavior still remain unclear. Especially the reason for the decreasing response on supposedly coated and pure platinum surfaces would need more throughout inspection. Furthermore, the results presented in this work point out that in amperometric biosensors one of the first requirements is to produce continuous and homogeneous coating on the sensor surface. The layer should also be thick enough to enable the verification of its properties. As seen from the commercial sensors by Pinnacle it is possible to create such coatings with appropriate reproducibility. However, the polymer layers on the electrode inflict a problem on the storage stability of the sensors. In *in vivo* applications there is usually no need to dry the sensors within their operational life, but, on the contrary, in *in vitro* experiments where biosensors is for example combined with some other sampling method it may be necessary to perform several consecutive measurements with different intervals. In addition to neuroscience, amperometric biosensors are utilized for example in the detection of pesticides and storing the sensors at dry room temperature without loosing the performance significantly would provide the possibility to perform the experiments also in field conditions.

It is clear that the examination presented here is still incomplete. The main obstacle is the unknown structure of the polymeric layers deposited both on self-made and Pinnacle sensors. Without proper knowledge of the properties of these materials it is impossible to form a complete analysis of the electrochemical phenomena on the

electrode surfaces. For example, it would be beneficial to obtain more information about the electrochemical processes in the layers.

Most importantly, an often neglected aspect in development of biosensors is the difference between conducting *in vitro* and *in vivo* experiments. There are several studies published yearly where the authors have shown the operation of their sensors *in vitro* but still to date there are only a couple of commercial sensor application in the market. In this work it was acknowledged that the Pinnacle sensor optimized to work *in vivo* did produce a response to glutamate at higher concentrations than 10 μM which is, however, 100 times higher than the actual limit of detection given by the sensor provider. This demonstrates the importance of taking the final operational environment into account in the development process as early as possible.

References

[1] S.F. Cogan. Neural stimulation and recording electrodes. *Annual Review of Biomedical Engineering*, 10:275–309, 2008.

[2] J.S. Perlmutter and J.W. Mink. Deep Brain Stimulation. *Annual Review of Neuroscience*, 29:229–257, 2006.

[3] A.J. Bard and L.R. Faulkner. *Electrochemical Methods: Fundamentals and applications*. Wiley, 2nd edition, 2000.

[4] A.C. Michael and L.M. Borland. *Electrochemical Methods for Neuroscience*. CRC Press, 2007.

[5] D.L. Robinson, A. Hermans, A.T. Seipel, and R.M. Wightman. Monitoring rapid chemical communication in the brain. *Chemical reviews*, 108(7):2554, 2008.

[6] L. Murtomäki, T. Kallio, R. Lahtinen, and K. Kontturi. *Sähkökemia*. Teknillinen korkeakoulu, 2010.

[7] D.R Thévenot, K. Toth, R. A Durst, G. S Wilson, et al. Electrochemical biosensors: Recommended definitions and classification. Technical report, International Union of Pure and Applied Chemistry, 1999.

[8] C.N. Kotanen, F.G. Moussy, S. Carrara, and A. Guiseppi-Elie. Implantable enzyme amperometric biosensors. *Biosensors and Bioelectronics*, 35(1):14–26, 2012.

[9] M.S. Gazzaniga, R.B. Ivry, and G.R. Mangun. *The cognitive neuroscience: The biology of the mind*. W.W. Norton & Company, Inc., 2nd edition, 2002.

[10] M. Perry, Q. Li, and R.T. Kennedy. Review of recent advances in analytical techniques for the determination of neurotransmitters. *Analytica Chimica Acta*, 653(1):1–22, 2009.

[11] Y.-H. Jo and R. Schlichter. Synaptic corelease of ATP and GABA in cultured spinal neurons. *Nature Neuroscience*, 2(3):241–245, 1999.

[12] H. Bult, G.E. Boeckxstaens, P.A. Pelckmans, F.H. Jordaens, Y.M. Van Maercke, and A.G. Herman. Nitric oxide as an inhibitory non-adrenergic non-cholinergic neurotransmitter. *Nature*, 345(6273):346–347, 1990.

[13] M. N. Friedemann, S. W. Robinson, and G. A. Gerhardt. O-phenylenediamine-modified carbon fiber electrodes for the detection of nitric oxide. *Analytical Chemistry*, 68(15):2621–2628, 1996.

[14] B. Belsham. Glutamate and its role in psychiatric illness. *Human Psychopharmacology: Clinical and Experimental*, 16(2):139–146, 2001.

[15] G.l Riede, B. Platt, and J. Micheau. Glutamate receptor function in learning and memory. *Behavioural Brain Research*, 140:1–47, 2003.

[16] D. Attwell. Brain uptake of glutamate: Food for thought. *The Journal of Nutrition*, 130(4):1023S–1025S, 2000.

[17] C.M. Anderson and R.A. Swanson. Astrocyte glutamate transport: Review of properties, regulation, and physiological functions. *Glia*, 32(1):1–14, 2000.

[18] M. Ankarcrona, J.M. Dypbukt, E. Bonfoco, B. Zhivotovsky, S. Orrenius, S.A. Lipton, and P. Nicotera. Glutamate-induced neuronal death: A succession of necrosis or apoptosis depending on mitochondrial function. *Neuron*, 15(4):961–973, 1995.

[19] M. Takahashi, B. Billups, D. Rossi, M. Sarantis, M. Hamann, and D. Attwell. The role of glutamate transporters in glutamate homeostasis in the brain. *Journal of Experimental Biology*, 200(2):401–409, 1997.

[20] J. Théberge, R. Bartha, D.J. Drost, R.S. Menon, A. Malla, J. Takhar, R.W. Neufeld, J. Rogers, W. Pavlosky, B. Schaefer, et al. Glutamate and glutamine measured with 4.0 T proton MRS in never-treated patients with schizophrenia and healthy volunteers. *American Journal of Psychiatry*, 159(11):1944–1946, 2002.

[21] N. Fayed, P. J. Modrego, G. Rojas-Salinas, and K. Aguilar. Brain glutamate levels are decreased in Alzheimer's disease: A magnetic resonance spectroscopy study. *American Journal of Alzheimer's Disease and Other Dementias*, 26(6):450–456, 2011.

[22] B. K. Day, F. Pomerleau, J. J. Burmeister, P. Huettl, and G. A. Gerhardt. Microelectrode array studies of basal and potassium-evoked release of L-glutamate in the anesthetized rat brain. *Journal of Neurochemistry*, 96(6):1626–1635, 2006.

[23] G.W. Wilson and R. Gifford. Biosensors for real-time *in vivo* measurements. *Biosensors and Bioelectronics*, 20(12):2388–2403, 2005.

[24] R.T. Kennedy, Thompson J. E., and T.W. Vickroy. In vivo monitoring of amino acids by direct sampling of brain extracellular fluid at ultralow flow rates and capillary electrophoresis. *Journal of Neuroscience Methods*, 114(1):39–49, 2002.

[25] S. Parrot, L. Bert, L. Mouly-Badina, V. Sauvinet, J. Colussi-Mas, L. Lambas-Senas, F. Robert, J.-P. Bouilloux, M.-F. Suaud-Chagny, L. Denoroy, and B. Renaud. Microdialysis monitoring of catecholamines and excitatory amino acids in the rat and mouse brain: Recent developments based on capillary electrophoresis with laser-induced fluorescence detection - A mini-review. *Cellular and Molecular Neurobiology*, 23(4-5):793–804, 2003.

[26] M.W. Lada, T.W. Vickroy, and R.T. Kennedy. High temporal resolution monitoring of glutamate and aspartate *in vivo* using microdialysis on-line with capillary electrophoresis with laser-induced fluorescence detection. *Analytical Chemistry*, 69(22):4560–4565, 1997.

[27] Y. Okubo, H. Sekiya, S. Namiki, H. Sakamoto, S. Iinuma, M. Yamasaki, M. Watanabe, K. Hirose, and M. Iino. Imaging extrasynaptic glutamate dynamics in the brain. *Proceedings of the National Academy of Sciences*, 107(14):6526–6531, 2010.

[28] S.l A. Hires, Y. Zhu, and R. Y. Tsien. Optical measurement of synaptic glutamate spillover and reuptake by linker optimized glutamate-sensitive fluorescent reporters. *Proceedings of the National Academy of Sciences*, 105(11):4411–4416, 2008.

[29] W. Tan, V. Parpura, P.G. Haydon, and E.S. Yeung. Neurotransmitter imaging in living cells based on native fluorescence detection. *Analytical Chemistry*, 67(15):2575–2579, 1995.

[30] K. Deisseroth. Controlling the brain with light. *Scientific American*, 303(5):48–55, 2010.

[31] K. Deisseroth. Optogenetics. *Nature Methods*, 8(1):26–29, 2011.

[32] P.A. Kottke, C. Kranz, Y.K. Kwon, J.-F. Masson, B. Mizaikoff, and A.G. Fedorov. Theory of polymer entrapped enzyme ultramicroelectrodes: Fundamentals. *Journal of Electroanalytical Chemistry*, 612(2):208–218, 2008.

[33] N. Dale, S. Hatz, F. Tian, and E. Llaudet. Listening to the brain: microelectrode biosensors for neurochemicals. *Trends in Biotechnology*, 23(8):420–428, 2005.

[34] L.C. Clark Jr. and C. Lyons. Electrode systems for continuous monitoring in cardiovascular surgery. *Annals of the New York Academy of Sciences*, 102:29–45, 1962.

[35] J.J. Burmeister and G.A. Gerhardt. Ceramic-based multisite microelectrode arrays for in vivo electrochemical recordings of glutamate and other neurochemicals. *TrAC - Trends in Analytical Chemistry*, 22(9):498–502, 2003.

[36] S. Chakraborty and C.R. Raj. Amperometric biosensing of glutamate using carbon nanotube based electrode. *Electrochemistry Communications*, 9(6):1323–1330, 2007.

[37] Y. Xiao, C. Cui, J.M. Hancock, M. Bouguettaya, J.R. Reynolds, and D.C. Martin. Electrochemical polymerization of poly(hydroxymethylated-3,4-ethylenedioxythiophene) (PEDOT-MeOH) on multichannel neural probes. *Sensors and Actuators B: Chemical*, 99:437–443, 2004.

[38] R.D. O'Neill, S.-C. Chang, J.P. Lowry, and C.J. McNeil. Comparisons of platinum, gold, palladium and glassy carbon as electrode materials in the design of biosensors for glutamate. *Biosensors and Bioelectronics*, 19(11):1521–1528, 2004.

[39] S. Sotiropoulou, V. Gavalas, V. Vamvakaki, and N.A. Chaniotakis. Novel carbon materials in biosensor systems. *Biosensors and Bioelectronics*, 18:211–215, 2003.

[40] S. Qin, M. Van der Zeyden, W.H. Oldenziel, T.I.F.H. Cremers, and B.H.C. Westerink. Microsensors for*in vivo* measurement of glutamate in brain tissue. *Sensors*, 8(11):6860–6884, 2008.

[41] J.J. Gooding, M. Hämmerle, and E.A.H. Hall. An enzyme electrode with response independent of the thickness of the enzyme layer. *Sensors and Actuators B: Chemical*, 34:516–523, 1996.

[42] C.P. McMahon, G. Rocchitta, P.A. Serra, S.M. Kirwan, J.P. Lowry, and R.D. O'Neill. The efficiency of immobilised glutamate oxidase decreases with surface enzyme loading: An electrostatic effect, and reversal by a polycation significantly enhances biosensor sensitivity. *Analyst*, 131(1):68–72, 2006.

[43] A. Sassolas, L.J. Blum, and B.D. Leca-Bouvier. Immobilization strategies to develop enzymatic biosensors. *Biotechnology Advances*, 30(3):489–511, 2012.

[44] J.M. Cooper, P.L. Foreman, A. Glidle, T.W. Ling, and D.J. Pritchard. Glutamate oxidase enzyme electrodes: microsensors for neurotransmitter determination using electrochemically polymerized permselective films. *Journal of Electroanalytical Chemistry*, 388:143–149, 1995.

[45] C. Debiemme-Chouvy. A very thin overoxidized polypyrrole membrane as coating for fast time response and selective H_2O_2 amperometric sensor. *Biosensors and Bioelectronics*, 25(11):2454–2457, 2010.

[46] E. Naylor, D.V. Aillon, S. Gabbert, H. Harmon, D.A. Johnson, G.S. Wilson, and P.A. Petillo. Simultaneous real-time measurement of EEG/EMG and L-glutamate in mice: A biosensor study of neuronal activity during sleep. *Journal of Electroanalytical Chemistry*, 656:106–113, 2011.

[47] H. Ernst and M. Knoll. Electrochemical characterisation of uric acid and ascorbic acid at a platinum electrode. *Analytica Chimica Acta*, 449(1-2):129–134, 2001.

[48] K. Rekha, M.D. Gouda, M.S. Thakur, and N.G. Karanth. Ascorbate oxidase based amperometric biosensor for organophosphorous pesticide monitoring. *Biosensors and Bioelectronics*, 15:499–502, 2000.

[49] J.C. Deutsch. Dehydroascorbic acid. *Journal of Chromatography A*, 881:299–307, 2000.

[50] J.C. Deutsch. Ascorbic acid oxidation by hydrogen peroxide. *Analytical Biochemistry*, 255(1):1–7, 1998.

[51] N. Wisniewski, F. Moussy, and W.M. Reichert. Characterization of implantable biosensor membrane biofouling. *Fresenius' Journal of Analytical Chemistry*, 366(6-7):611–621, 2000.

[52] N. Wisniewski and M. Reichert. Methods for reducing biosensor membrane biofouling. *Colloids and Surfaces B: Biointerfaces*, 18:197–219, 2000.

[53] B.D. Ratner, A.S. Hoffman, F.J. Schoen, and J. E. Lemons, editors. *Biomaterials science : An introduction to materials in medicine.* Academic Press, San Diego CA, 2nd edition, 2004.

[54] P.A. Kottke, C. Kranz, Y.K. Kwon, J.-F. Masson, B. Mizaikoff, and A.G. Fedorov.

[55] P.N. Bartlett and D.J. Caruana. Electrochemical immobilization of enzymes Part VI. Microelectrodes for the detection of L-lactate based on flavocytochrome b2 immobilized in a poly(phenol) film. *Analyst*, 119(2):175–180, 1994.

[56] N. Martens and E.A.H. Hall. Model for an immobilized oxidase enzyme electrode in the presence of two oxidants. *Analytical Chemistry*, 66(17):2763–2770, 1994.

[57] M. Somasundrum and K. Aoki. The steady-state current at microcylinder electrodes modified by enzymes immobilized in conducting or non-conducting material. *Journal of Electroanalytical Chemistry*, 530(1-2):40–46, 2002.

[58] S.B. Hall, E.A. Khudaish, and A.L. Hart. Electrochemical oxidation of hydrogen peroxide at platinum electrodes. Part 1. An adsorption-controlled mechanism. *Electrochimica Acta*, 43(5-6):579–588, 1997.

[59] S.B. Hall, E.A. Khudaish, and A.L. Hart. Electrochemical oxidation of hydrogen peroxide at platinum electrodes. Part II: Effect of potential. *Electrochimica Acta*, 43(14-15):2015–2024, 1998.

[60] S.B. Hall, E.A. Khudaish, and A.L. Hart. Electrochemical oxidation of hydrogen peroxide at platinum electrodes. Part III: Effect of temperature. *Electrochimica Acta*, 44(14):2455–2462, 1999.

[61] S.B. Hall, E.A. Khudaish, and A.L. Hart. Electrochemical oxidation of hydrogen peroxide at platinum electrodes. Part IV: Phosphate buffer dependence. *Electrochimica Acta*, 44(25):4573–4582, 1999.

[62] S.B. Hall, E.A. Khudaish, and A.L. Hart. Electrochemical oxidation of hydrogen peroxide at platinum electrodes. Part V: Inhibition by chloride. *Electrochimica Acta*, 45(21):3573–3579, 2000.

[63] F.C. Anson. Chemical evidence for oxide films on platinum electrometric electrodes. *Journal of the American Chemical Society*, 79(18):4901–4904, 1957.

[64] O. Kotiranta. Amperometrisen välittäjäaineanturin karakterisointilaitteiston suunnittelu ja toteutus. Master's thesis, Aalto University, 2012.

[65] Discussion with Mr. Peter Petillo from Pinnacle Technology Inc. on 20.5.2013.

[66] A. Hickling and W. Wilson. The anodic decomposition of hydrogen peroxide. *J. Electrochem. Soc.*, 98:425–433, 1951.

[67] Y.-F. Yang and G. Denuault. Scanning electrochemical microscopy (SECM): Study of the formation and reduction of oxides on platinum electrode surfaces in Na2SO4 solution (pH = 7). *Journal of Electroanalytical Chemistry*, 443(2):273–282, 1998.

[68] S. Wachiratianchai, A. Bhumiratana, and S. Udomsopagit. Isolation, purification, and characterization of L-glutamate oxidase from Streptomyces sp. 18G. *Electronic Journal of Biotechnology*, 7(3):274–281, 2004.